IEEE Access
Multidisciplinary | Rapid Review | Open Access Journal

Received October 16, 2018, accepted October 31, 2018, date of publication December 10, 2018,
date of current version January 7, 2019.

Digital Object Identifier 10.1109/ACCESS.2018.2885247

In-Band Full-Duplex Relay-Assisted Millimeter-Wave System Design

DEEPA JAGYASI, (Student Member, IEEE), AND P. UBAIDULLA, (Senior Member, IEEE)
Signal Processing and Communication Research Center, International Institute of Information Technology, Hyderabad 500032, India

Corresponding author: Deepa Jagyasi (jagyasi.deepa@research.iiit.ac.in)

This work was supported by the Visvesvaraya Young Faculty Research Fellowship of the Ministry of Electronics and Information Technology (MeitY), Government of India.

ABSTRACT Millimeter-wave (mmWave) communication is a promising technology for future wireless systems due to the availability of huge unlicensed bandwidth. However, the need for large number of radio frequency (RF) chains associated with the antenna array and the corresponding increase in hardware complexity and power consumption are major stumbling blocks to its implementability. In this paper, we propose a low-complexity in-band full-duplex relay-assisted mmWave communication system design. We obtain the proposed multiple-input multiple-output analog–digital hybrid transceivers and relay filters by minimizing the overall sum-mean-square-error while mitigating the effect of residual loopback self-interference (LSI) in the system. The number of RF chains required in the proposed design is less than the number of antennas. We first present a design assuming the availability of perfect channel state information (CSI) at all the nodes. Later, we extend it to a robust design assuming a more realistic scenario, where the available CSI is imperfect. Furthermore, the LSI channel knowledge is assumed to be imperfect for both the designs rendering them robust to errors in loopback CSI. We employ sparse approximation technique to reduce the hardware complexity in the proposed system designs. The proposed algorithms are shown to converge to a limit even though the global convergence is hard to prove since the overall problem is non-convex. The hardware complexity-performance tradeoff of the proposed design is analyzed. Furthermore, the resilience of the robust design in the presence of CSI errors and the performance of both the proposed designs over various parameters are illustrated via numerical simulations.

INDEX TERMS Full-duplex, hybrid beamforming, millimeter-wave communication, residual self-interference, robust design.

I. INTRODUCTION

Millimeter Wave (mmWave) communication, with its potential to exploit the huge unlicensed and under-exploited spectrum, has been recognized as a promising technique to solve the unprecedented challenge of ever increasing data traffic for next generation cellular networks. mmWave frequency band (30-300 GHz) offers wide bandwidth that can accommodate many more users as compared to current cellular bands. However, signal propagation at these frequencies experience severe challenges like penetration loss, higher free-scale path loss, oxygen absorption, and rain fading [1]–[3]. Some of these challenges can be tackled by means of high beamforming gains achievable with antenna arrays consisting of large number of elements [3], [4]. An upside of the mmWave frequency band is the shorter wavelength that enables packing of large number of antenna elements in small volumes. Hence, large multiple-input-multiple-output (MIMO) will be a key technique in mmWave systems. At mmWave frequencies, however, the large number of mixed signal components associated with each antenna element increases the cost and power consumption of the system. Thus, it is infeasible to adopt the fully-digital beamforming architecture where an individual radio frequency (RF) chain is dedicated to each antenna. As such, it is imperative to reduce the overall hardware complexity by reducing the total number of RF chains in mmWave system design in order to make it practically implementable for future networks. One possible solution is the analog-digital hybrid architecture, wherein an individual RF chain is associated with each sub-array of antennas rather than a single antenna [5]. Recently, many efficient hybrid structures have been reported in [6]–[13]. In [6], over-sampling codebook based hybrid minimum

sum-mean-square-error precoding scheme has been discussed for three-dimensional MIMO systems. Wideband hybrid precoding schemes using principal component analysis have been discussed in [7] for backhaul/fronthaul links. In [8]–[13], various hybrid systems designed by using spatially sparse coding techniques have been discussed for large MIMO mmWave systems.

Even though the problem of severe path loss in mmWave signals can be tackled by achieving high beamforming gain using massive MIMO at the transceivers, long-distance communication is another major challenge for these systems. mmWave communication is sensitive to non-line-of-sight (NLoS) scenarios due to huge penetration loss caused by blockages [4]. Hence, relay-assisted mmWave communication systems can be utilized for increasing the overall communication range, link quality, and reliability. mmWave systems with relays have been proposed in the literature for various communication scenarios including cellular communication [14], [15], device-to-device communication [16], and indoor applications [17]. Relay-assisted systems have been vastly studied for wireless communication [18]–[21]. Regenerative and non-regenerative relays are two type of relaying strategies in general [18]–[20]. Conventionally, relay-assisted wireless communication systems operate in half-duplex (HD) mode, wherein the transmission and reception take place in separate time slots or frequency sub-bands. mmWave cooperative systems with HD relays have been studied in [10], [11], and [22]–[24]. A two-way HD amplify-forward (AF) relay-based system has been presented in [10] and [11], wherein the transceiver and relay filters are obtained by solving sum-mean-square-error (SMSE) optimization problem for mmWave channel. In [22], a joint design to obtain precoder and relay filter matrices by considering the sum-rate maximization problem has been studied for mmWave systems with single as well as multiple relay nodes operating in HD mode. In [23] and [24], hybrid beamforming scheme for an HD relay-assisted mmWave system with multiple receivers has been proposed.

Full-duplex (FD) communication, with its potential for better spectral efficiency compared to HD, is regarded as another promising technology for next generation networks. In-band FD relay systems have gained tremendous interest amongst researchers as they combine the benefits of both HD and one-way FD systems [25], [26]. With in-band FD relaying operation, signal transmission and reception take place simultaneously over the same frequency channel without increasing the bandwidth usage. FD relay-assisted mmWave communication systems have been reported in [27] and [28]. Wei *et al.* [27] presented an overview of the challenges and solutions in terms of energy-efficiency for a FD relay-assisted mmWave system. Later in [28], an FD relay-based system has been proposed for mmWave backhaul links while considering the sum-rate maximization problem. However, in-band FD mode of communication that uses the same frequency channel for transmission as well as reception introduces loopback self-interference (LSI), which is the transmitted signal received at its local receiver node. Furthermore, the LSI accumulates over time thus degrading the performance of the system drastically. Hence, mitigation of LSI is a major challenge in the design of in-band FD system. Recent developments in fabricating a non-reciprocal circulator using transistors [29] can reduce the effect of LSI on the system. LSI cancellation techniques for in-band FD relays operating in microwave frequency ranges have been reported in [30] and [31]. However, very small distance among antenna elements in mmWave system leads to significantly higher LSI as compared to systems operating in microwave ranges. Recently, LSI cancellation techniques for mmWave systems have been discussed in [32]. However, complete elimination of the LSI is not possible with the currently available techniques and we are left with residual LSI at each FD node. This residual LSI, which accumulates over time, will further degrade the overall system performance.

In this paper, we propose hybrid transceiver and relay filter designs for an in-band FD two-way AF relay-assisted mmWave system. All the nodes are equipped with multiple antennas and operate in full-duplex mode. The works cited above assume the availability of perfect channel state information (CSI) at all transceivers nodes. However, the CSI available with the system is not always perfect due to various factors such as estimation error, feedback delays, quantization errors, pilot contamination, etc., which can introduce errors. Hence, the transceivers that are designed assuming the availability of perfect CSI are not likely to achieve the desired performance in the presence of CSI errors. Effect of imperfect CSI on the performance of MIMO systems is discussed in [33]. Thus in practice, the systems that are resilient to such errors are highly desirable. Robust designs that take into account the imperfections in the available channel knowledge for different systems have been discussed in [34]–[38]; but to the best of authors' knowledge, robust designs for FD relay-based mmWave systems have not been reported yet. The full-duplex system considered in this paper employs existing LSI cancellation techniques. However, complete LSI cancellation is not possible and all the nodes suffer from residual LSI. This residual LSI effect can be modeled in terms of imperfections in the CSI of the loop-back channels [39], [40]. This further motivates us to design robust transceiver algorithms that are resilient to erroneous CSI in mmWave FD relay-based systems by taking into consideration the imperfections in available channel knowledge. We propose transceiver and relay filter design applicable in two different scenarios depending on the channels for which CSI error is significant. First, we consider the scenario, where the CSI of all the links except the loopback channels are perfectly known. Next, we consider the case, where the available CSI of all the channels are imperfect. In both the cases, the adverse effect of the CSI error on the system performance is mitigated by proper precoder, receiver, and relay filter matrix design. Moreover, as discussed previously,

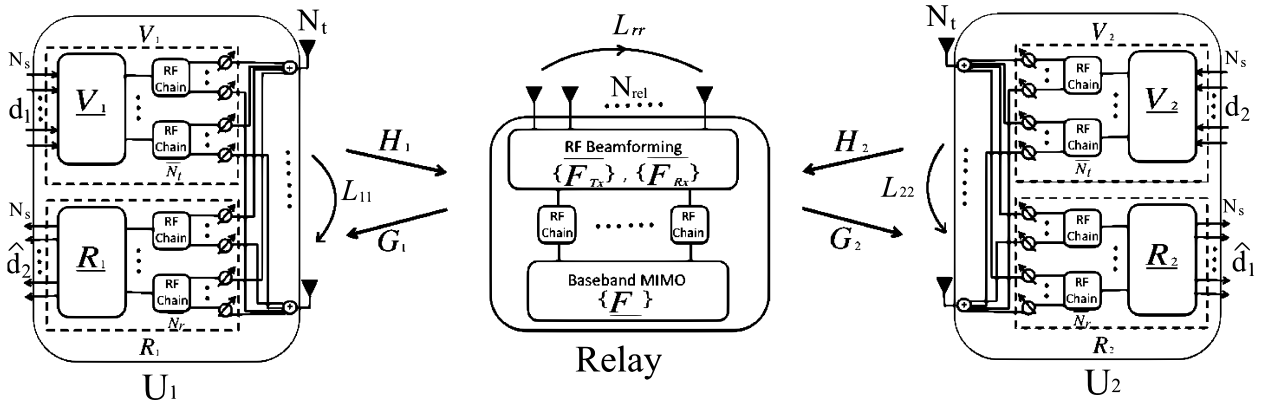

FIGURE 1. Hybrid FD two-way relay-assisted mmWave communication system.

signals propagating at mmWave frequencies suffer severe path loss [4], [41]. Path loss model for mmWave frequencies have been studied in [42]. We employ a similar mmWave path loss model in our proposed design.

The main contributions of this paper can be summarized as follows:

- We first jointly design the optimal transceiver and relay filter matrices for a mmWave full-duplex two-way relay network by minimizing the sum-mean-square-error assuming the availability of perfect CSI of all the links except the loopback channel.
- We extend it further to a robust design for the case, where the available CSI of all the links are imperfect, by taking into account the imperfections hence rendering the performance resilient to errors in the CSI.
- The detrimental effects of the residual LSI at transceiver and relay nodes are mitigated by considering it in the overall system design.
- We further decompose these optimal matrices into analog-digital hybrid filters by using orthogonal matching pursuit (OMP) algorithm and thus achieving reduced hardware complexity of the overall system.

We carry out the performance evaluation of the proposed schemes with extensive simulations over various parameter values and demonstrate the comparison results later in the paper.

The rest of this paper is organized as follows. System and channel model is described in Sec. II. The proposed FD system design considering the availability of perfect channel knowledge is discussed in Sec. III. In Sec. IV, low-complexity hybrid transceiver and relay filter design is described. Sec. V describes the robust FD system design. Sec. VI presents the simulation results and finally, Sec. VII concludes this paper.

Notations: Throughout this paper, we use lowercase letters to denote scalar values, bold-faced lowercase letters to denote column vectors and bold-faced uppercase letters to denote matrices. $\underline{x}$, $\underline{\mathbf{X}}$ and $\overline{x}$, $\overline{\mathbf{X}}$ imply that the variable x and matrix $\mathbf{X}$ correspond to the baseband and RF block, respectively. For any matrix $\mathbf{X}$, $tr(\mathbf{X})$, $\mathbf{E}\{\mathbf{X}\}$, $\mathbf{X}^H$, $\mathbf{X}^T$, $vec(\mathbf{X})$, $mat(\mathbf{X})$, $\|\mathbf{X}\|_0$, $\|\mathbf{X}\|_F$, and $det(\mathbf{X})$ denote trace, expectation, conjugate transpose, transpose, vectorization, matricization, 0-norm, Frobenius-norm, and determinant operator, respectively. For any matrices $\mathbf{X}$ and $\mathbf{Y}$, $\mathbf{X} \otimes \mathbf{Y}$ represents the Kronecker product. We represent any matrix $\mathbf{X}$ that belongs to robust scheme by $\mathbf{X}'$. x_k, $\mathbf{x}_k$, and $\mathbf{X}_k$ denote a scalar, a vector, and a matrix, respectively, for k^{th} user at time t. The timeslot index $t-1$ is denoted by τ throughout this paper. $x_{k,j}$, $\mathbf{x}_{k,j}$, and $\mathbf{X}_{k,j}$ define a scalar, a vector, and a matrix, respectively, for the k^{th} user at time j, where $k \in \{1, 2\}$. k denotes the other user, *i.e.*, when $k = 1$, $k = 2$ and *vice versa*.

II. SYSTEM AND CHANNEL MODEL

A. SYSTEM MODEL

We consider a hybrid mmWave wireless communication system with two users ($U1$ and $U2$) and a non-regenerative two-way relay, all operating in full-duplex mode as shown in Fig. 1. We assume that there is no direct link between the users and they communicate only via the relay node. The total number of antenna elements associated with each user and relay node for transmission as well as reception are N_t and N_{rel}, respectively. In a fully-digital precoding/receive filtering system, an individual RF chain is associated with each antenna element. On the other hand, in an analog-digital hybrid processing system, the antenna elements are grouped into subarrays and an individual RF chain is associated with each subarray. The hardware complexity of a hybrid system is thus lower than the corresponding fully-digital system. The symbol vector transmitted by the k^{th} user/transceiver, $U_k, k = 1, 2$, is denoted by $\mathbf{d}_k \in \mathbf{C}^{N_s \times 1}$ with $N_s < N_t$. The number of RF chains associated with the users and the relay node for employing hybrid processing is $\overline{N}_t$ and $\overline{N}_{rel}$, respectively, such that $N_s < \overline{N}_t \leq N_t$ and $\overline{N}_{rel} \leq N_{rel}$. Let $\mathbf{V}_k$ and $\mathbf{R}_k$ denote the optimal fully-digital precoder and receive filter matrices, respectively, at the k^{th} user terminal and let $\mathbf{F}$ denote the optimal fully-digital relay gain filter matrix. Then, in the corresponding analog-digital hybrid transmit precoder, $\mathbf{d}_k$ is processed by a digital baseband precoder matrix $\underline{\mathbf{V}}_k \in \mathbf{C}^{\overline{N}_t \times N_s}$ followed by an RF precoder

denoted by the matrix $\overline{\mathbf{V}}_k \in \mathbf{C}^{N_t \times \overline{N}_t}$, such that the matrix $\mathbf{V}_k$ is effectively decomposed as $\overline{\mathbf{V}}_k \underline{\mathbf{V}}_k$. Similarly, the relay node processes the received signal by an RF beamformer $\overline{\mathbf{F}}_{Rx} \in \mathbf{C}^{\overline{N}_{rel} \times N_{rel}}$ followed by a digital baseband relay gain matrix $\underline{\mathbf{F}} \in \mathbf{C}^{\overline{N}_{rel} \times \overline{N}_{rel}}$ and an RF transmit beamformer $\overline{\mathbf{F}}_{Tx} \in \mathbf{C}^{N_{rel} \times \overline{N}_{rel}}$ such that the product $\overline{\mathbf{F}}_{Tx}\underline{\mathbf{F}}\overline{\mathbf{F}}_{Rx}$ is equivalent to the fully-digital relay precoder matrix $\mathbf{F}$. The received signals at the transceivers are processed by RF beamformer matrix $\overline{\mathbf{R}}_k \in \mathbf{C}^{N_t \times \overline{N}_t}$ followed by the baseband combiner matrix $\underline{\mathbf{R}}_k \in \mathbf{C}^{\overline{N}_t \times N_s}$ in order to generate the effect of the fully-digital receive matrix $\mathbf{R}_k$.

The information exchange between the users take place in two time slots. In time slot $t = 0$, both the users transmit their data and the relay node receives these signals. The relay node then multiplies the received signal with a relay gain matrix and transmits the resultant signal in slot $t = 1$. Moreover, in the same time slot $t = 1$, the users receive the signal transmitted by the relay and simultaneously transmit next data symbols, which are then received by the relay node. Thus, the overall FD operation is functional only from time slot $t = 1$ onwards. The signal received by the relay node in time slot $t = 0$ is given by

$$\mathbf{y}_{r,0} = \mathbf{H}_{1,0}\mathbf{V}_{1,0}\mathbf{d}_{1,0} + \mathbf{H}_{2,0}\mathbf{V}_{2,0}\mathbf{d}_{2,0} + \mathbf{n}_r, \tag{1}$$

where $\mathbf{H}_{k,i}$ is the channel gain matrix from the k^{th} user to the relay (forward channel), $\mathbf{V}_{k,i}$ is the precoder matrix at the k^{th} user, $\mathbf{d}_{k,i}$ is the symbol vector transmitted by the k^{th} user, all in the i^{th} time slot, and $\mathbf{n}_r$ is a zero-mean additive white Gaussian noise vector at the relay node with covariance matrix $\sigma^2_{n_r}\mathbf{I}$. In the next time slot, the signal transmitted by relay is given by

$$\begin{aligned}\mathbf{x}_{r,1} &= \mathbf{F}_1\mathbf{y}_{r,0}, \\ &= \mathbf{F}_1\mathbf{H}_{1,0}\mathbf{V}_{1,0}\mathbf{d}_{1,0} + \mathbf{F}_1\mathbf{H}_{2,0}\mathbf{V}_{2,0}\mathbf{d}_{2,0} + \mathbf{F}_1\mathbf{n}_r,\end{aligned} \tag{2}$$

where $\mathbf{F}_i$ is the relay gain matrix in the i^{th} time slot. In the same time slot (*i.e.,* at $t = 1$), the users precode and transmit the symbol vectors and receive the signals from the relay simultaneously. The signal received by the k^{th} user can be written as

$$\mathbf{y}_{k,1} = \mathbf{G}_{k,1}\mathbf{x}_{r,1} + \mathbf{L}_{k,1}\mathbf{V}_{k,1}\mathbf{d}_{k,1} + \mathbf{n}_k, \quad k = 1, 2, \tag{3}$$

where $\mathbf{G}_{k,j}$ is the channel gain matrix from the relay to the k^{th} user (reverse channel), $\mathbf{L}_{k,j}$ is the loopback channel gain matrix of the k^{th} user in the j^{th} time slot, and $\mathbf{n}_k$ is the zero-mean additive white Gaussian noise vector with covariance matrix $\sigma^2_{n_k}\mathbf{I}$. Owing to two-way relaying, the signal received by each user contains a term involving the symbol transmitted by it in the previous slot. However, this self-interference can be completely removed since the users have perfect knowledge of the relevant CSI. The simultaneous transmission and reception in the FD mode introduces the LSI at all the nodes. Let $\mathbf{L}_{k,j}$ and $\mathbf{L}_{r,j}$ be the loop-back channel matrices at k^{th} user and the relay node, respectively, in the j^{th} time slot. We assume that the available CSI for loop-back channel is imperfect such that

$$\mathbf{L}_{i,j} = \widehat{\mathbf{L}}_{i,j} + \boldsymbol{\Upsilon}_{i,j}, \quad i = 1, 2, r,$$

where $\widehat{\mathbf{L}}_{i,j}$ is the available loop-back channel estimate and $\boldsymbol{\Upsilon}_{i,j} \sim \mathcal{N}(0, \sigma^2_{e_{i,j}}\mathbf{I})$ denotes the corresponding error in the available CSI. The error variance can be determined based on the technique used for the CSI estimation [43]. Thus, the signal by the k^{th} user in time slot $t = 1$, after canceling the relay-induced self-interference, can be expressed as

$$\begin{aligned}\mathbf{y}_{k,1} = \mathbf{G}_{k,1}\mathbf{F}_1\mathbf{H}_{k,0}\mathbf{V}_{k,0}\mathbf{d}_{k,1} + \mathbf{G}_{k,1}\mathbf{F}_1\mathbf{n}_r + \widehat{\mathbf{L}}_{k,1}\mathbf{x}_{k,1} \\ + \boldsymbol{\Upsilon}_{k,1}\mathbf{x}_{k,1} + \mathbf{n}_k,\end{aligned} \tag{4}$$

where $\mathbf{x}_{k,j} = \mathbf{V}_{k,j}\mathbf{d}_{k,j}$. Since the available loop-back channel information is imperfect, complete LSI cancellation is not possible and a residual LSI remains at the nodes. The resultant received signal after LSI cancellation in time slot $t = 1$ at the k^{th} user can be written as

$$\mathbf{y}_{k,1} = \mathbf{G}_{k,1}\mathbf{F}_1\mathbf{H}_{k,0}\mathbf{V}_{k,0}\mathbf{d}_{k,0} + \mathbf{G}_{k,1}\mathbf{F}_1\mathbf{n}_r + \boldsymbol{\Upsilon}_{k,1}\mathbf{x}_{k,1} + \mathbf{n}_k, \tag{5}$$

where $\boldsymbol{\Upsilon}_{k,1}\mathbf{x}_{k,1}$ is the residual LSI. Similarly, the signal received by the relay in time slot $t = 1$, after LSI cancellation, can be written as

$$\mathbf{y}_{r,1} = \mathbf{H}_{1,1}\mathbf{V}_{1,1}\mathbf{d}_{1,1} + \mathbf{H}_{2,1}\mathbf{V}_{2,1}\mathbf{d}_{2,1} + \boldsymbol{\Upsilon}_{r,1}\mathbf{x}_{r,1} + \mathbf{n}_r, \tag{6}$$

where $\boldsymbol{\Upsilon}_{r,1}\mathbf{x}_{r,1}$ is the residual LSI. The relaying operation leads to the accumulation of the residual LSI over time. Proceeding from (6) recursively, the received signal at the relay in any time slot $t \geq 1$, after the interference cancellation, can be expressed as

$$\mathbf{y}_{r,t} = \mathbf{H}_{1,t}\mathbf{V}_{1,t}\mathbf{d}_{1,t} + \mathbf{H}_{2,t}\mathbf{V}_{2,t}\mathbf{d}_{2,t} + \boldsymbol{\zeta}_t + \mathbf{n}_r, \tag{7}$$

where $\boldsymbol{\zeta}_t$, the cumulative residual LSI at the relay, is given by

$$\boldsymbol{\zeta}_t = \sum_{i=0}^{t-1} \Big\{ \prod_{j=1}^{t-i} (\boldsymbol{\Upsilon}_{r,t-j}\mathbf{F}_{t-j})(\mathbf{H}_{1,i}\mathbf{V}_{1,i}\mathbf{d}_{1,i} + \mathbf{H}_{2,i}\mathbf{V}_{2,i}\mathbf{d}_{2,i} + \mathbf{n}_r) \Big\}. \tag{8}$$

As the FD operation starts only from $t = 1$, the residual LSI starts accumulating from $t = 1$ and at any time t, $\boldsymbol{\zeta}$ can be considered as the cumulative effect of LSI from the current and all previous time slots.

Henceforth, we will use the symbol τ to denote the time slot $t - 1$ for any $t \geq 1$. Moreover, the variables will have explicit time slot index only if they do not correspond to the current slot t. Thus, the signal transmitted by the relay in time slot t is given by

$$\mathbf{x}_r = \mathbf{F}\mathbf{y}_{r,\tau}, \tag{9}$$

and the signal received by the k^{th} user in time slot t is given by

$$\begin{aligned}\mathbf{y}_k = \mathbf{G}_k\mathbf{F}\mathbf{H}_{k,\tau}\mathbf{V}_{k,\tau}\mathbf{d}_{k,\tau} + \mathbf{G}_k\mathbf{F}\mathbf{n}_r + \boldsymbol{\Upsilon}_k\mathbf{V}_k\mathbf{d}_k \\ + \mathbf{G}_k\mathbf{F}\boldsymbol{\zeta} + \mathbf{n}_k, \quad k = 1, 2.\end{aligned} \tag{10}$$

B. CHANNEL MODEL

Due to high free-space path loss and the use of large number of tightly-packed antennas at mmWave frequencies, we adopt a narrow-band parametric clustered channel model. We consider the extended Saleh-Valenzuela model [41], in which the generalized channel matrix $\mathbf{C}$ from a transmitter equipped with N_T transmit antennas to a receiver equipped with N_R receive antennas is modeled as

$$\mathbf{C} = \varrho\left(\gamma \sum_{m=1}^{N_{cl}} \sum_{n=1}^{N_{ray}} \alpha_{m,n} \mathbf{a}_R(\theta_{m,n,j}) \mathbf{a}_T(\phi_{m,n,k})^H\right), \tag{11}$$

where ϱ represents the path loss and other variables are as described below. The variable N_{ray} represents the number of rays in each of N_{cl} clusters and the normalization factor $\gamma = \sqrt{\frac{N_T N_R}{N_{cl} N_{ray}}}$ is chosen such that $E\left[||\mathbf{C}||_F^2\right] = N_T N_R$. The zero-mean complex Gaussian random variable $\alpha_{m,n}$ with variance σ_α^2 denotes the gain of n^{th} ray in m^{th} cluster. The array response vectors at the transmitter and the receiver are denoted by $\mathbf{a}_T(\phi_{m,n})$ and $\mathbf{a}_R(\theta_{m,n})$, respectively, where ϕ is the azimuthal angle of departure (AoD) and θ is the azimuthal angle of arrival (AoA). We consider a uniform linear array (ULA) antenna structure such that

$$\mathbf{a}_T(\theta) = \frac{1}{\sqrt{N}}\begin{bmatrix} 1 & \exp^{i\beta\sin(\theta)} \cdots \exp^{i(N_T-1)\beta\sin(\theta)} \end{bmatrix}^T,$$
$$\mathbf{a}_R(\phi) = \frac{1}{\sqrt{N}}\begin{bmatrix} 1 & \exp^{i\beta\sin(\phi)} \cdots \exp^{i(N_R-1)\beta\sin(\phi)} \end{bmatrix}^T,$$

where $\beta = \frac{2\pi d}{\lambda}$, d is the inter-element distance, $i = \sqrt{-1}$, and λ is the wavelength. The azimuth angles ϕ and θ follow Laplacian distribution and the mean angle of each cluster follows uniform distribution over $(-\pi, \pi)$. In the simulation experiments, we employ the following mmWave path loss model [42]:

$$\varrho = 20\log_{10}\left(\frac{4\pi l_0}{\lambda}\right) + n10\log_{10}\left(\frac{l}{l_0}\right) + X_\sigma. \tag{12}$$

where l_0 is the close-in free-space reference distance considered to be 5 meters for mmWave system, l is the distance between transmitter and receiver, λ is the operating wavelength in mmWave frequency band, n is the average path loss coefficient, and X_σ is a shadowing Gaussian random variable with zero mean and standard deviation σ.

III. JOINT TRANSCEIVER AND RELAY FILTER DESIGN

In this section, we present an FD two-way AF relay-assisted mmWave communication system design assuming the availability of perfect knowledge of forward and reverse channel state information. We assume that the available loopback CSI is imperfect. We jointly design the fully-digital transceiver $\{\mathbf{V}_k, \mathbf{R}_k\}$ and relay filter $\mathbf{F}$ by minimizing the SMSE ε under a constraint on the total relay transmit power:

$$\min_{\tilde{\mathbf{F}}, \mathbf{V}_1, \mathbf{V}_2, \mathbf{R}_1, \mathbf{R}_2, \alpha} \quad \varepsilon$$
$$\text{subject to: } \mathbf{E}\left[||\mathbf{x}_r||^2\right] \le P_T, \tag{13}$$

where P_T is the upper limit on the relay transmit power. In the proposed design, detrimental effect of the residual LSI on the system performance is minimized by incorporating it in the SMSE. For ease of derivation, we write the relay filter matrix as $\mathbf{F} = \alpha\tilde{\mathbf{F}}$, where the scaling factor α is chosen such that $||\tilde{\mathbf{F}}||_F = 1$. Moreover, we scale the received signal by α^{-1} in order to ensure a closed-form solution for the relay filter matrix $\mathbf{F}$. With this modification, we can now express the SMSE, $\varepsilon(\alpha, \mathbf{V}_1, \mathbf{V}_2, \mathbf{R}_1, \mathbf{R}_2, \tilde{\mathbf{F}})$, at time slot t, as follows:

$$\begin{aligned}
&\varepsilon(\alpha, \mathbf{V}_1, \mathbf{V}_2, \mathbf{R}_1, \mathbf{R}_2, \tilde{\mathbf{F}}) \\
&= \mathbf{E}\left[||\mathbf{d}_{2,\tau} - \alpha^{-1}\mathbf{R}_1^H\mathbf{y}_1||^2\right] \\
&\quad + \mathbf{E}\left[||\mathbf{d}_{1,\tau} - \alpha^{-1}\mathbf{R}_2^H\mathbf{y}_2||^2\right] \\
&= N_s(P_1+P_2) - tr(\mathbf{R}_2^H\mathbf{G}_2\tilde{\mathbf{F}}\mathbf{H}_{1,\tau}\mathbf{V}_{1,\tau} \\
&\quad + \mathbf{V}_{1,\tau}^H\mathbf{H}_{1,\tau}^H\tilde{\mathbf{F}}^H\mathbf{G}_2^H\mathbf{R}_2 \\
&\quad + \mathbf{R}_1^H\mathbf{G}_1\tilde{\mathbf{F}}\mathbf{H}_{2,\tau}\mathbf{V}_{2,\tau} + \mathbf{V}_{2,\tau}^H\mathbf{H}_{2,\tau}^H\tilde{\mathbf{F}}^H\mathbf{G}_1^H\mathbf{R}_1) \\
&\quad + \alpha^{-2}\left(\sigma_{n_1}^2 + \sigma_{e_1}^2 tr(\mathbf{V}_1\mathbf{V}_1^H)\right)tr(\mathbf{R}_1\mathbf{R}_1^H) + \alpha^{-2}\left(\sigma_{n_2}^2\right. \\
&\quad \left. + \sigma_{e_2}^2 tr(\mathbf{V}_2\mathbf{V}_2^H)\right)tr(\mathbf{R}_2\mathbf{R}_2^H) + tr(\mathbf{R}_1^H\mathbf{G}_1\tilde{\mathbf{F}}\mathbf{Z}_1\tilde{\mathbf{F}}^H\mathbf{G}_1^H\mathbf{R}_1) \\
&\quad + tr(\mathbf{R}_2^H\mathbf{G}_2\tilde{\mathbf{F}}\mathbf{Z}_2\tilde{\mathbf{F}}^H\mathbf{G}_2^H\mathbf{R}_2),
\end{aligned} \tag{14}$$

where P_1 and P_2 denote transmit power of users $U1$ and $U2$, respectively, and

$$\mathbf{Z}_1 = \mathbf{\Psi} + \sigma_{n_r}^2\mathbf{I}_{n_r} + \mathbf{H}_{2,\tau}\mathbf{V}_{2,\tau}\mathbf{V}_{2,\tau}^H\mathbf{H}_{2,\tau}^H,$$
$$\mathbf{Z}_2 = \mathbf{\Psi} + \sigma_{n_r}^2\mathbf{I}_{n_r} + \mathbf{H}_{1,\tau}\mathbf{V}_{1,\tau}\mathbf{V}_{1,\tau}^H\mathbf{H}_{1,\tau}^H,$$

with $\mathbf{\Psi} = \mathbf{E}[\boldsymbol{\zeta}\boldsymbol{\zeta}^H]$. The term $\mathbf{\Psi}$, which captures the average effect of the cumulative LSI at the relay, can be expressed as

$$\begin{aligned}
\mathbf{\Psi} = \mathbf{E}\Bigg[\sum_{i=0}^{t-1}\Bigg\{\prod_{j=1}^{t-i}(\mathbf{\Upsilon}_{r,t-j}\mathbf{F}_{t-j})(\widehat{\mathbf{H}}_{1,i}\mathbf{V}_{1,i}\mathbf{V}_{1,i}^H\widehat{\mathbf{H}}_{1,i}^H \\
+ \sigma_{n_r}^2\mathbf{I}_{n_r} + \widehat{\mathbf{H}}_{2,i}\mathbf{V}_{2,i}\mathbf{V}_{2,i}^H\widehat{\mathbf{H}}_{2,i}^H)\prod_{j=1}^{t-i}(\mathbf{F}_{t-j}^H\mathbf{\Upsilon}_{r,t-j}^H)\Bigg\}\Bigg].
\end{aligned}$$

Having developed the expression for the SMSE, we now turn our attention to the transmit power constraint in (13). The total relay transmit power can be expressed as

$$\mathbf{E}\left[||\mathbf{x}_r||^2\right] = \mathbf{E}\left[tr(\mathbf{x}_r\mathbf{x}_r^H)\right] = \alpha^2 tr(\tilde{\mathbf{F}}\mathbf{Z}_r\tilde{\mathbf{F}}^H), \tag{15}$$

where,

$$\mathbf{Z}_r = \mathbf{\Psi} + \sigma_{n_r}^2\mathbf{I}_{n_r} + \widehat{\mathbf{H}}_{1,\tau}\mathbf{V}_{1,\tau}\mathbf{V}_{1,\tau}^H\widehat{\mathbf{H}}_{1,\tau}^H + \widehat{\mathbf{H}}_{2,\tau}\mathbf{V}_{2,\tau}\mathbf{V}_{2,\tau}^H\widehat{\mathbf{H}}_{2,\tau}^H.$$

We can now solve the optimization problem given in (13) to obtain the optimal transceiver and relay filter matrices. Based on the solution presented in Appendix VII, for given values of transceiver precoder and receive filter matrices, we have

$$\begin{aligned}
\tilde{\mathbf{F}} &= mat\left(\mathbf{O}^{-1}vec(\widehat{\mathbf{G}}_2^H\mathbf{R}_2\mathbf{V}_{1,\tau}^H\widehat{\mathbf{H}}_{1,\tau}^H + \widehat{\mathbf{G}}_1^H\mathbf{R}_1\mathbf{V}_{2,\tau}^H\widehat{\mathbf{H}}_{2,\tau}^H)\right), \\
\alpha &= \sqrt{N_{rel}P_T\left(tr(\tilde{\mathbf{F}}\mathbf{Z}_r\tilde{\mathbf{F}}^H)\right)^{-1}},
\end{aligned} \tag{16}$$

where,

$$\mathbf{O} = (\mathbf{Z}_1^T \otimes \widehat{\mathbf{G}}_1^H \mathbf{R}_1 \mathbf{R}_1^H \widehat{\mathbf{G}}_1^H) + (\mathbf{Z}_2^T \otimes \widehat{\mathbf{G}}_2^H \mathbf{R}_2 \mathbf{R}_2^H \widehat{\mathbf{G}}_2^H) + \Big(\mathbf{Z}_r^T \otimes (\frac{A}{P_T})\mathbf{I}\Big),$$

$$A = \sum_{i=1}^{K} \big(\sigma_{n_i}^2 + \sigma_{e_i}^2 tr(\mathbf{V}_i \mathbf{V}_i^H)\big) tr(\mathbf{R}_i \mathbf{R}_i^H).$$

Hence, we can obtain the relay filter matrix as

$$\mathbf{F} = \alpha \tilde{\mathbf{F}}. \tag{17}$$

Similarly, for given values of $\mathbf{R}_k$ and $\mathbf{F}$, the precoder matrices are given by

$$\mathbf{V}_{k,\tau} = \Big[\widehat{\mathbf{H}}_{k,\tau}^H \tilde{\mathbf{F}}^H \widehat{\mathbf{G}}_k^H \mathbf{R}_k \mathbf{R}_k^H \widehat{\mathbf{G}}_k \tilde{\mathbf{F}} \widehat{\mathbf{H}}_{k,\tau} + (\frac{A}{P_T}) \widehat{\mathbf{H}}_{k,\tau}^H \tilde{\mathbf{F}}^H \tilde{\mathbf{F}} \widehat{\mathbf{H}}_{k,\tau} \Big]^{-1} \widehat{\mathbf{H}}_{k,\tau}^H \tilde{\mathbf{F}}^H \widehat{\mathbf{G}}_k^H \mathbf{R}_k, \ k = 1, 2, \tag{18}$$

and receive filter matrices, for given values of $\mathbf{V}_k$ and $\mathbf{F}$, are given by

$$\mathbf{R}_k = \Big[\alpha^{-2}(\sigma_{n_k}^2 + \sigma_{e_k}^2 tr(\mathbf{V}_k \mathbf{V}_k^H))\mathbf{I} + \widehat{\mathbf{G}}_k \tilde{\mathbf{F}} \mathbf{Z}_k \tilde{\mathbf{F}}^H \widehat{\mathbf{G}}_k^H \Big]^{-1} \widehat{\mathbf{G}}_k \tilde{\mathbf{F}} \widehat{\mathbf{H}}_{k,\tau} \mathbf{V}_{k,\tau}. \tag{19}$$

TABLE 1. Proposed iterative algorithm.

Iterative algorithm for computing $\mathbf{F}$, $\mathbf{V}$, and $\mathbf{R}$ that minimize SMSE
Initialize $\mathbf{F}$, $\mathbf{V}_k$ and $\mathbf{R}_k$, $\forall k \in \{1,2\}$, set convergence threshold Λ and ϵ_0
Iteration index $n = 1$
Repeat
1. Update $\tilde{\mathbf{F}}$ by using $\mathbf{R}_k$, $\mathbf{V}_{k,\tau}$ and $\mathbf{V}_k$, $\forall k \in \{1,2\}$
2. Update α by using $\tilde{\mathbf{F}}$
3. Update $\mathbf{F}$ by using $\tilde{\mathbf{F}}$ and $\boldsymbol{\alpha}$
4. Update $\mathbf{R}_k$ by using $\mathbf{F}$, $\mathbf{V}_{k,\tau}$ and $\mathbf{V}_k$, $\forall k \in \{1,2\}$
5. Update $\mathbf{V}_k$ by using $\mathbf{F}$ and $\mathbf{R}_k$, $\forall k \in \{1,2\}$
6. Calculate ε_n by using $\mathbf{F}$, $\mathbf{V}_k$ and $\mathbf{R}_k$, $\forall k \in \{1,2\}$; $n = n+1$;
Until $\lvert\epsilon_n - \epsilon_{n-1}\rvert \leqslant \theta$

It can be observed that the optimization problem in (13) is non-convex. Hence, we obtain the optimal values of the individual variables, i.e., (17), (18), and (19), iteratively through coordinate descent method as given in Table 1. Let ϵ_j be the value of the objective function in the j^{th} iteration. Since ϵ_j is the value of an MSE function, its always non-negative. Furthermore, due to the minimization process in each iteration, we have $\epsilon_{j+1} \leq \epsilon_j$, $\forall j$. The sequence $\{\epsilon_j\}$ is convergent since it is bounded below and monotonically decreasing with j. However, global convergence is not guaranteed since the original problem is not convex. Simulation results showing the convergence behavior of the proposed algorithms are discussed in Sec. VI. For the given algorithm, the iterations can be stopped whenever the absolute difference of ϵ_j and ϵ_{j+1} falls below a suitable threshold. Once we obtain the optimal transceiver and relay filter matrices, we adopt hybrid architecture by decomposing these filters into digital baseband and analog RF beamforming matrices. The hybrid filters thus designed achieve reduced hardware complexity in the overall mmWave system.

IV. LOW-COMPLEXITY ANALOG-DIGITAL HYBRID FILTER DESIGN

In this section, we describe the design of hybrid precoder, receive filter, and relay gain filter for the proposed mmWave communication systems. The key problem here is to obtain the baseband digital and RF beamforming matrices that jointly approximate the matrix corresponding to the fully-digital processing. In order to achieve this, we decompose the previously obtained optimal matrices $\mathbf{V}_k$, $\mathbf{R}_k$, and $\mathbf{F}$, into their corresponding hybrid processors using the OMP-based sparse approximation technique.

A. HYBRID PRECODER/RECEIVE FILTER DESIGN

Orthogonal matching pursuit algorithm has been extensively studied and is used in various signal processing applications [5], [44], [45]. Given the optimal fully-digital precoders ($\mathbf{V}_k$) and receive filters ($\mathbf{R}_k$), we obtain the hybrid processors by decomposing the optimal matrices into their corresponding RF and baseband hybrid filters using OMP-based sparse approximation technique. OMP is a greedy approach and in the current application, it iteratively computes the RF and baseband matrices. We elaborate this process in the following.

In general, the optimal MMSE receive filter for the k^{th} user can be rewritten as,

$$\mathbf{R}_k = \alpha {\boldsymbol{\Gamma}_{\mathbf{y}_k}}^{-1} \boldsymbol{\Gamma}_{\mathbf{y}_k \mathbf{d}_{k,\tau}}, \tag{20}$$

where $\boldsymbol{\Gamma}_{\mathbf{y}_k} = \mathbf{E}[\mathbf{y}_k \mathbf{y}_k^H]$, $\boldsymbol{\Gamma}_{\mathbf{y}_k \mathbf{d}_k} = \mathbf{E}[\mathbf{y}_k \mathbf{d}_{k,\tau}^H]$. Similarly, in case of hybrid system, the baseband receive filter matrix $\underline{\mathbf{R}}_k$, for a given RF beamformer matrix $\overline{\mathbf{R}}_k$, is given by

$$\underline{\mathbf{R}}_k = \boldsymbol{\Gamma}_{\mathbf{z}_k}^{-1} \boldsymbol{\Gamma}_{\mathbf{z}_k \mathbf{d}_{k,\tau}} = (\overline{\mathbf{R}}_k^H \boldsymbol{\Gamma}_{\mathbf{y}_k} \overline{\mathbf{R}}_k)^{-1} \overline{\mathbf{R}}_k^H \boldsymbol{\Gamma}_{\mathbf{y}_k \mathbf{d}_{k,\tau}}, \tag{21}$$

where $\mathbf{z}_k$ is the received signal at the baseband processor, $\boldsymbol{\Gamma}_{\mathbf{z}_k} = \mathbf{E}[\mathbf{z}_k \mathbf{y}_k^H]$, and $\boldsymbol{\Gamma}_{\mathbf{z}_k \mathbf{d}_{k,\tau}} = \mathbf{E}[\mathbf{z}_k \mathbf{d}_{k,\tau}^H]$. The OMP sparse problem for the receiver can be formulated as

$$\overline{\mathbf{R}}_k = \arg \min_{\overline{\mathbf{R}}_k} \mathbf{E} \| \mathbf{d}_{k,\tau} - \underline{\mathbf{R}}_k{}^H \overline{\mathbf{R}}_k \mathbf{y}_k \|^2. \tag{22}$$

Using [12, Lemma-I], this optimization problem can be reformulated as

$$\overline{\mathbf{R}}_k = \arg \min_{\overline{\mathbf{R}}_k} \| \boldsymbol{\Gamma}_{\mathbf{y}_k}^{\frac{1}{2}} \mathbf{R}_k - \boldsymbol{\Gamma}_{\mathbf{y}_k}^{\frac{1}{2}} \overline{\mathbf{R}}_k \underline{\mathbf{R}}_k \|_F^2. \tag{23}$$

Introducing a dictionary $\mathbf{S}_{BF} \in \mathbf{C}^{N_t \times N_t}$, we design the RF beamformer by selecting $\overline{N}_t$ candidate vectors from $\boldsymbol{\Gamma}_{\mathbf{y}_k}^{\frac{1}{2}} \mathbf{S}_{BF}$ that are strongly correlated to the residue updated at each iteration. Depending on performance and complexity characteristics, we can consider various predefined dictionaries such as set of eigen beamformers, discrete Fourier transform (DFT) beamformers, discrete cosine transform (DCT) beamformers, discrete Hadamard transform (DHT) beamformers, or antenna selection. Given the dictionary $\mathbf{S}_{BF}$, the baseband receive filter matrix is obtained by choosing corresponding $\overline{N}_t$ non-zero rows from the solution of the following

sparse approximation problem:

$$\ddot{\underline{\mathbf{R}}}_k = \arg\min_{\ddot{\underline{\mathbf{R}}}_k} \|\mathbf{\Gamma}_{\mathbf{y}_k}^{\frac{1}{2}}\mathbf{R}_k - \mathbf{\Gamma}_{\mathbf{y}_k}^{\frac{1}{2}}\mathbf{S}_{BF}\ddot{\underline{\mathbf{R}}}_k\|_F^2$$
$$\text{subject to} : \|\text{diag}\,(\ddot{\underline{\mathbf{R}}}_k\ddot{\underline{\mathbf{R}}}_k^H)\|_0 = \overline{N}_r. \quad (24)$$

In order to obtain the hybrid precoder matrices, we consider a dual system, where the precoder of original system acts as receiver. Following the same procedure as above, we can then obtain the hybrid baseband and RF precoder matrices by formulating and solving optimization problems as follows:

$$\overline{\mathbf{V}}_k = \arg\min_{\overline{\mathbf{V}}_k} \|\mathbf{\Gamma}_{\mathbf{y}_k^r}^{\frac{1}{2}}\mathbf{V}_k - \mathbf{\Gamma}_{\mathbf{y}_k^r}^{\frac{1}{2}}\overline{\mathbf{V}}_k\underline{\mathbf{V}}_k\|_F^2, \quad (25)$$

$$\ddot{\underline{\mathbf{V}}}_k = \arg\min_{\mathbf{V}_k} \|\mathbf{\Gamma}_{\mathbf{y}_k^r}^{\frac{1}{2}}\mathbf{V}_k - \mathbf{\Gamma}_{\mathbf{y}_k^r}^{\frac{1}{2}}\mathbf{S}_{BF}\ddot{\underline{\mathbf{V}}}_k\|_F^2,$$
$$\text{s.t.}\ \|\text{diag}(\ddot{\underline{\mathbf{V}}}_k\ddot{\underline{\mathbf{V}}}_k^H)\|_0 = \overline{N}_t \text{ and } \|\mathbf{S}_{BF}\ddot{\underline{\mathbf{V}}}_k\|_F^2 = \|\mathbf{V}_k\|_F^2, \quad (26)$$

where $\mathbf{y}_k^r$ is the signal received by the beamformer in the dual system and $\mathbf{S}_{BF}$ is the dictionary. The generalized algorithm to obtain hybrid precoder and receive filter matrices is given in Table. 2. In this algorithm, the RF beamforming matrix is selected from the set of candidate vectors $\mathbf{S}_{BF}$ and baseband matrices are obtained by minimizing the effective residue $\mathbf{A}_i$ in each iteration. We hence obtain $\{\underline{\mathbf{V}}_k, \overline{\mathbf{V}}_k\}$ and $\{\underline{\mathbf{R}}_k, \overline{\mathbf{R}}_k\}$ filters from the generalized algorithm by passing the appropriate parameters.

TABLE 2. Hybrid precoder and receive filter design.

OMP-based algorithm for hybrid precoder and receive filter design
Initializations:
Hybrid precoder: $\mathbf{W}_k = \mathbf{V}_k, \mathbf{\Phi} = \mathbf{\Gamma}_{\mathbf{y}_k^r}, \overline{\mathbf{Q}} = \overline{\mathbf{V}}$, and $\underline{\mathbf{Q}} = \underline{\mathbf{V}}$.
Hybrid receive filter: $\mathbf{W}_k = \mathbf{R}_k, \mathbf{\Phi} = \mathbf{\Gamma}_{\mathbf{y}_k}, \overline{\mathbf{Q}} = \overline{\mathbf{R}}$, and $\underline{\mathbf{Q}} = \underline{\mathbf{R}}$.
$\overline{\mathbf{Q}}_k = [\,]$.
$\mathbf{A}_0 = \mathbf{W}_k$.
for $i = 1$ to $\overline{N}_t$ do
$\mathbf{\Lambda}_{i-1} = (\mathbf{\Phi}^{\frac{1}{2}}\mathbf{S}_{BF})^H(\mathbf{\Phi}^{\frac{1}{2}}\mathbf{A}_{i-1})$.
$l = arg\,max_{m=1\ldots N_t}(\mathbf{\Lambda}_{i-1}\mathbf{\Lambda}_{i-1}^H)_{m,m}$.
$\overline{\mathbf{Q}}_k = [\overline{\mathbf{Q}}_k|(\mathbf{\Phi}^{\frac{1}{2}}\mathbf{S}_{BF})(:,l)]$.
$\underline{\mathbf{Q}}_k = (\overline{\mathbf{Q}}_k^H\mathbf{\Phi}\overline{\mathbf{Q}}_k)^{-1}\overline{\mathbf{Q}}_k^H\mathbf{\Phi}\mathbf{W}_k$.
$\mathbf{A}_i = \frac{\mathbf{W}_k - \overline{\mathbf{Q}}_k\underline{\mathbf{Q}}_k}{\|\mathbf{W}_k - \overline{\mathbf{Q}}_k\underline{\mathbf{Q}}_k\|_F}$.
end for.
$\underline{\mathbf{Q}} = \sqrt{N_s}\frac{\underline{\mathbf{Q}}}{\|\overline{\mathbf{Q}}\underline{\mathbf{Q}}^H\|_F}$.
Return $\overline{\mathbf{Q}}, \underline{\mathbf{Q}}$.

B. HYBRID AF FULL-DUPLEX RELAY FILTER DESIGN

The optimal relay gain matrix $\mathbf{F}$ is decomposed into hybrid matrices $\overline{\mathbf{F}}_{Tx}$, $\underline{\mathbf{F}}$, and $\overline{\mathbf{F}}_{Rx}$ such that $||\mathbf{F} - \overline{\mathbf{F}}_{Tx}\underline{\mathbf{F}}\overline{\mathbf{F}}_{Rx}||_F$ is minimized. Following the approach in [37], the hybrid relay filters can obtained by solving the following optimization problem:

$$(\overline{\mathbf{F}}_{Tx}, \underline{\mathbf{F}}, \overline{\mathbf{F}}_{Rx}) = \arg\min_{\overline{\mathbf{F}}_{Tx}, \underline{\mathbf{F}}, \overline{\mathbf{F}}_{Rx}} ||\mathbf{F} - \overline{\mathbf{F}}_{Tx}\underline{\mathbf{F}}\overline{\mathbf{F}}_{Rx}||_F$$
$$\text{s.t.}\ \overline{\mathbf{F}}_{Tx}^{(j)} \in \mathbf{S}_{Tx-BF}, (\overline{\mathbf{F}}_{Rx})^{(j)} \in \mathbf{S}_{Rx-BF},$$
$$||\overline{\mathbf{F}}_{Tx}\underline{\mathbf{F}}\overline{\mathbf{F}}_{Rx}||_F^2 = P_T. \quad (27)$$

where, the j^{th} column vector of the RF beamforming matrices $\overline{\mathbf{F}}_{Tx}$ and $\overline{\mathbf{F}}_{Rx}$ for transmitting and receiving signals, respectively, are jointly selected from a set of candidate vectors $\mathbf{S}_{Tx-BF}$ and $\mathbf{S}_{Rx-BF}$. When both the vectors are suitably selected, the effective residue is updated in each step after the corresponding baseband filter is obtained as a least-squares solution. Hence, the overall error is minimized with each iteration. The complete OMP-based algorithm for the obtaining the hybrid relay filters is given in Table 3.

TABLE 3. Hybrid relay filter design.

OMP-based algorithm for hybrid relay filter design
Require $\mathbf{F}, \mathbf{S}_{Rx-BF}, \mathbf{S}_{Tx-BF}$.
$\overline{\mathbf{F}}_{Rx} = \overline{\mathbf{F}}_{Tx} = [\,]$.
$\mathbf{F}_{res} = \mathbf{F}$.
for $i = 1$ to $\overline{N}_{rel}$ do
$\mathbf{\Lambda}_{Rx}^{i-1} = \mathbf{F}_{res}\mathbf{S}_{Rx-BF}^H$.
$q = arg\,max_{m=1\ldots N_{rel}}(\mathbf{\Lambda}_{Tx}^{i-1}(\mathbf{\Lambda}_{Tx}^{i-1})^H)_{m,m}$.
$\overline{\mathbf{F}}_{Rx} = [\overline{\mathbf{F}}_{Rx}^T|(\mathbf{S}_{Rx-BF}^T)(:,q)]^T$.
$\mathbf{\Lambda}_{Tx}^{i-1} = \mathbf{S}_{Tx-BF}^H\mathbf{F}_{res}\overline{\mathbf{F}}_{Rx}^H$.
$l = arg\,max_{m=1\ldots N_{rel}}(\mathbf{\Lambda}_{Rx}^{i-1}(\mathbf{\Lambda}_{Rx}^{i-1})^H)_{m,m}$.
$\overline{\mathbf{F}}_{Tx} = [\overline{\mathbf{F}}_{Tx}|\mathbf{S}_{Tx-BF}(:,l)]$.
$\underline{\mathbf{F}} = (\overline{\mathbf{F}}_{Tx}^H\overline{\mathbf{F}}_{Tx})^{-1}\overline{\mathbf{F}}_{Tx}^H\mathbf{F}\overline{\mathbf{F}}_{Rx}^H(\overline{\mathbf{F}}_{Rx}\overline{\mathbf{F}}_{Rx}^H)$.
$\mathbf{F}_{res} = \frac{\mathbf{F} - \overline{\mathbf{F}}_{Tx}\underline{\mathbf{F}}\overline{\mathbf{F}}_{Rx}}{||\mathbf{F} - \overline{\mathbf{F}}_{Tx}\underline{\mathbf{F}}\overline{\mathbf{F}}_{Rx}||_F}$.
end for.
return $\overline{\mathbf{F}}_{Tx}, \overline{\mathbf{F}}_{Rx}$, and $\underline{\mathbf{F}}$.

V. ROBUST TRANSCEIVER AND RELAY FILTER DESIGN

Due to various errors that can occur during channel estimation and feedback in any realistic system, availability of perfect channel knowledge is an idealistic assumption, which rarely holds in practice, especially in the case of large-scale MIMO systems. Such estimation errors will degrade the overall performance of the system. Thus, it is important to develop designs that are resilient to CSI imperfections. Here, we propose robust transceiver and relay filter design by taking into account the estimation errors in the forward and the reverse channels. We consider the following CSI error model:

$$\mathbf{H}_k' = \mathbf{H}_k + \mathbf{\Delta}_{\mathbf{H}_k}, \quad k = 1, 2, \quad (28)$$

where $\mathbf{H}'_k$ is the true channel, $\mathbf{H}_k$ is the available CSI estimate of the forward link, and $\mathbf{\Delta}_{\mathbf{H}_k} \sim \mathcal{CN}(0, \sigma^2_{\mathbf{H}_k})$ denotes the corresponding error in the CSI. Similarly for the reverse link,

$$\mathbf{G}'_k = \mathbf{G}_k + \mathbf{\Delta}_{\mathbf{G}_k}, \quad k = 1, 2, \tag{29}$$

where $\mathbf{G}'_k$ is the true channel and $\mathbf{G}_k$ is the available CSI estimate of the reverse link, and $\mathbf{\Delta}_{\mathbf{G}_k} \sim \mathcal{CN}(0, \sigma^2_{\mathbf{G}_k})$ denotes the corresponding error. Incorporating the channel model described above, signal received by the relay at time t can be written as

$$\mathbf{y}_r = \mathbf{H}'_1\mathbf{V}_1\mathbf{d}_1 + \mathbf{H}'_2\mathbf{V}_2\mathbf{d}_2 + \boldsymbol{\zeta}' + \mathbf{n}_r, \tag{30}$$

where,

$$\begin{aligned}\boldsymbol{\zeta}' &= \sum_{i=0}^{t-1}\Big\{\prod_{j=1}^{t-i}(\mathbf{\Upsilon}_{r,t-j}\mathbf{F}_{t-j})(\mathbf{H}'_{1,i}\mathbf{V}_{1,i}\mathbf{d}_{1,i} + \mathbf{H}'_{2,i}\mathbf{V}_{2,i}\mathbf{d}_{2,i} \\ &\quad + \mathbf{n}_r)\Big\}. \\ &= \sum_{i=0}^{t-1}\Big\{\prod_{j=1}^{t-i}(\mathbf{\Upsilon}_{r,t-j}\mathbf{F}_{t-j})(\mathbf{H}_{1,i}\mathbf{V}_{1,i}\mathbf{d}_{1,i} + \mathbf{H}_{2,i}\mathbf{V}_{2,i}\mathbf{d}_{2,i} \\ &\quad + \mathbf{\Delta}_{\mathbf{H}_1,i}\mathbf{V}_{1,i}\mathbf{d}_{1,i} + \mathbf{\Delta}_{\mathbf{H}_2,i}\mathbf{V}_{2,i}\mathbf{d}_{2,i} + \mathbf{n}_r)\Big\}.\end{aligned} \tag{31}$$

The residual self-interference factor $\mathbf{\Psi}' = \mathbf{E}\{\boldsymbol{\zeta}'(\boldsymbol{\zeta}')^H\}$ for the robust design can be expressed as

$$\begin{aligned}\mathbf{\Psi}' &= \mathbf{E}\Big\{\sum_{i=0}^{t-1}\Big[\prod_{j=1}^{t-i}(\mathbf{\Upsilon}_{r,t-j}\mathbf{F}_{t-j})(\mathbf{H}_{1,i}\mathbf{V}_{1,i}\mathbf{V}^H_{1,i}\mathbf{H}^H_{1,i} \\ &\quad + \sigma^2_{H_1,i}\mathbf{V}_{1,i}\mathbf{V}^H_{1,i} + \sigma^2_{n_r}\mathbf{I} + \mathbf{H}_{2,i}\mathbf{V}_{2,i}\mathbf{V}^H_{2,i}\mathbf{H}^H_{2,i} \\ &\quad + \sigma^2_{H_2,i}\mathbf{V}_{2,i}\mathbf{V}^H_{2,i})\prod_{j=1}^{t-i}(\mathbf{F}^H_{t-j}\mathbf{\Upsilon}^H_{r,t-j})\Big]\Big\}, \\ &= \sigma^2_{e_r}\big[tr(\mathbf{H}_{1,\tau}\mathbf{V}_{1,\tau}\mathbf{V}^H_{1,\tau}\mathbf{H}^H_{1,\tau} + \sigma^2_{H_1,\tau}\mathbf{V}_{1,\tau}\mathbf{V}^H_{1,\tau} \\ &\quad + \sigma^2_{n_r}\mathbf{I} + \mathbf{H}_{2,\tau}\mathbf{V}_{2,\tau}\mathbf{V}^H_{2,\tau}\mathbf{H}^H_{2,\tau} + \sigma^2_{H_2,\tau}\mathbf{V}_{2,\tau}\mathbf{V}^H_{2,\tau})\mathbf{I} \\ &\quad + \mathbf{\Psi}'_\tau tr(\mathbf{F}_\tau\mathbf{F}^H_\tau)\big],\end{aligned} \tag{32}$$

where the expectation is with respect to all the CSI error variables. Furthermore, the SMSE and the relay transmit power are now random variables since they depend on the CSI error variables. Hence, we consider their expected values in the proposed robust design. The expected value of SMSE is given in (33), as shown at the bottom of this page. Thus, the design of fully-digital robust transceiver and relay filter that minimize SMSE under a constraint on the total relay transmit power can be formulated as

$$\min_{\tilde{\mathbf{F}},\mathbf{V}_1,\mathbf{V}_2,\mathbf{R}_1,\mathbf{R}_2,\alpha} \quad \varepsilon' \quad \text{s.t.: } \mathbf{E}\big[||\mathbf{x}'_r||^2_F\big] \le P_T. \tag{34}$$

The constraint function in the preceding optimization problem can be rewritten as

$$\mathbf{E}\big[||\mathbf{x}_r||^2_F\big] = \mathbf{E}\big[tr(\mathbf{x}_r\mathbf{x}^H_r)\big] = \alpha^2 tr(\tilde{\mathbf{F}}\mathbf{Z}'_r\tilde{\mathbf{F}}^H), \tag{35}$$

where,

$$\begin{aligned}\mathbf{Z}'_r &= \mathbf{\Psi}' + \mathbf{H}_{1,\tau}\mathbf{V}_{1,\tau}\mathbf{V}^H_{1,\tau}\mathbf{H}^H_{1,\tau} + \mathbf{H}_{2,\tau}\mathbf{V}_{2,\tau}\mathbf{V}^H_{2,\tau}\mathbf{H}^H_{2,\tau} \\ &\quad + \sigma^2_{H_2,\tau}tr(\mathbf{V}_{2,\tau}\mathbf{V}^H_{2,\tau})\mathbf{I} + \sigma^2_{H_1,\tau}tr(\mathbf{V}_{1,\tau}\mathbf{V}^H_{1,\tau})\mathbf{I} + \sigma^2_{n_r}\mathbf{I}_{n_r}.\end{aligned}$$

The robust design problem can be solved using the techniques presented in Appendix VII. Thus, given the robust precoder $\mathbf{V}_k$ and the receive filter $\mathbf{R}_k$, we can obtain the robust relay filter matrix as

$$\begin{aligned}\tilde{\mathbf{F}} &= mat\big(\mathbf{O}^{-1}vec(\mathbf{G}^H_2\mathbf{R}_2\mathbf{V}^H_{1,\tau}\mathbf{H}^H_{1,\tau} + \mathbf{G}^H_1\mathbf{R}_1\mathbf{V}^H_{2,\tau}\mathbf{H}^H_{2,\tau})\big), \\ \alpha &= \sqrt{N_{rel}P_T\big(tr(\tilde{\mathbf{F}}\mathbf{Z}'_r\tilde{\mathbf{F}}^H)\big)^{-1}},\end{aligned}$$

where,

$$\begin{aligned}\mathbf{O} &= (\mathbf{Z}'^T_1 \otimes \mathbf{G}^H_1\mathbf{R}_1\mathbf{R}^H_1\mathbf{G}^H_1) + (\mathbf{Z}'^T_2 \otimes \mathbf{G}^H_2\mathbf{R}_2\mathbf{R}^H_2\mathbf{G}^H_2) \\ &\quad + \big(\mathbf{Z}'^T_r \otimes (\frac{A}{P_T})\mathbf{I}\big) + \Big(\big(\mathbf{Z}'_2 + \sigma^2_{H_1,\tau}tr(\mathbf{V}_1\mathbf{V}^H_1)\mathbf{I}\big)^T \\ &\quad \otimes \sigma^2_{G_2}tr(\mathbf{R}_2\mathbf{R}^H_2)\mathbf{I}\Big) + \Big(\big(\mathbf{Z}'_1 + \sigma^2_{H_1,\tau}tr(\mathbf{V}_2\mathbf{V}^H_2)\mathbf{I}\big)^T \\ &\quad \otimes \sigma^2_{G_1}tr(\mathbf{R}_1\mathbf{R}^H_1)\mathbf{I}\Big),\end{aligned}$$

and,

$$\begin{aligned}A &= \Big[\big(\sigma^2_{n_1} + \sigma^2_{e_1}tr(\mathbf{V}_1\mathbf{V}^H_1)\big)tr(\mathbf{R}_1\mathbf{R}^H_1) \\ &\quad + \big(\sigma^2_{n_2} + \sigma^2_{e_2}tr(\mathbf{V}_2\mathbf{V}^H_2)\big)tr(\mathbf{R}_2\mathbf{R}^H_2)\Big].\end{aligned}$$

Hence, the robust relay filter matrix is obtained as

$$\mathbf{F} = \alpha\tilde{\mathbf{F}}. \tag{36}$$

$$\begin{aligned}\varepsilon' &= N_s(P_1 + P_2) - tr(\mathbf{R}^H_2\mathbf{G}_2\tilde{\mathbf{F}}\mathbf{H}_{1,\tau}\mathbf{V}_{1,\tau} + \mathbf{V}^H_{1,\tau}\mathbf{H}^H_{1,\tau}\tilde{\mathbf{F}}^H\mathbf{G}^H_2\mathbf{R}_2 + \mathbf{R}^H_1\mathbf{G}_1\tilde{\mathbf{F}}\mathbf{H}_{2,\tau}\mathbf{V}_{2,\tau} + \mathbf{V}^H_{2,\tau}\mathbf{H}^H_{2,\tau}\tilde{\mathbf{F}}^H\mathbf{G}^H_1\mathbf{R}_1) \\ &\quad + \alpha^{-2}\big(\sigma^2_{n_1} + \sigma^2_{e_1}tr(\mathbf{V}_1\mathbf{V}^H_1)\big)tr(\mathbf{R}_1\mathbf{R}^H_1) + \alpha^{-2}\big(\sigma^2_{n_2} + \sigma^2_{e_2}tr(\mathbf{V}_2\mathbf{V}^H_2)\big)tr(\mathbf{R}_2\mathbf{R}^H_2) + tr(\mathbf{R}^H_1\mathbf{G}_1\tilde{\mathbf{F}}\mathbf{Z}'_1\tilde{\mathbf{F}}^H\mathbf{G}^H_1\mathbf{R}_1) \\ &\quad + \sigma^2_{G_1}tr\Big(\tilde{\mathbf{F}}\big(\mathbf{Z}'_1 + \sigma^2_{H_2,\tau}tr(\mathbf{V}_{2,\tau}\mathbf{V}^H_{2,\tau})\mathbf{I}\big)\tilde{\mathbf{F}}^H\Big)tr(\mathbf{R}_1\mathbf{R}^H_1) + tr(\mathbf{R}^H_2\mathbf{G}_2\tilde{\mathbf{F}}\mathbf{Z}'_2\tilde{\mathbf{F}}^H\mathbf{G}^H_2\mathbf{R}_2) \\ &\quad + \sigma^2_{G_2}tr\Big(\tilde{\mathbf{F}}\big(\mathbf{Z}'_2 + \sigma^2_{H_1,\tau}tr(\mathbf{V}_{1,\tau}\mathbf{V}^H_{1,\tau})\mathbf{I}\big)\tilde{\mathbf{F}}^H\Big)tr(\mathbf{R}_2\mathbf{R}^H_2),\end{aligned} \tag{33}$$

where

$$\mathbf{Z}'_1 = \mathbf{\Psi}' + \sigma^2_{n_r}\mathbf{I}_{n_r} + \mathbf{H}_{2,\tau}\mathbf{V}_{2,\tau}\mathbf{V}^H_{2,\tau}\mathbf{H}^H_{2,\tau}, \quad \text{and} \quad \mathbf{Z}'_2 = \mathbf{\Psi}' + \sigma^2_{n_r}\mathbf{I}_{n_r} + \mathbf{H}_{1,\tau}\mathbf{V}_{1,\tau}\mathbf{V}^H_{1,\tau}\mathbf{H}^H_{1,\tau}.$$

Similarly, given the robust $\mathbf{F}$ and $\mathbf{R}_k$, the robust fully-digital precoder matrix for the k^{th} user is given by

$$\begin{aligned}\mathbf{V}_{k,\tau} = \Big[&\mathbf{H}_{k,\tau}^H \tilde{\mathbf{F}}^H \mathbf{G}_k^H \mathbf{R}_k \mathbf{R}_k^H \mathbf{G}_k \tilde{\mathbf{F}} \mathbf{H}_{k,\tau} \\ &+ \sigma_{H_k,\tau}^2 \sigma_{G_k}^2 tr(\tilde{\mathbf{F}}^H \tilde{\mathbf{F}}) tr(\mathbf{R}_k \mathbf{R}_k^H) \mathbf{I} \\ &+ \sigma_{G_k}^2 tr(\mathbf{R}_k \mathbf{R}_k^H) \mathbf{H}_{k,\tau}^H \tilde{\mathbf{F}}^H \tilde{\mathbf{F}} \mathbf{H}_{k,\tau} \\ &+ (\frac{A}{P_T}) \big(\mathbf{H}_{k,\tau}^H \tilde{\mathbf{F}}^H \tilde{\mathbf{F}} \mathbf{H}_{k,\tau} + \sigma_{H_k,\tau}^2 tr(\tilde{\mathbf{F}}^H \tilde{\mathbf{F}}) \mathbf{I}\big) \Big]^{-1} \\ &\times \mathbf{H}_{k,\tau}^H \tilde{\mathbf{F}}^H \mathbf{G}_k^H \mathbf{R}_k. \end{aligned} \tag{37}$$

Finally, for given values of robust $\mathbf{V}_k$ and $\mathbf{F}$, the robust receive filter at k^{th} user is given by

$$\begin{aligned}\mathbf{R}_k = \Big[&\alpha^{-2}\big(\sigma_{n_k}^2 + \sigma_{e_k}^2 tr\big(\mathbf{V}_k \mathbf{V}_k^H\big)\big)\mathbf{I} + \mathbf{G}_k \tilde{\mathbf{F}} \mathbf{Z}_k' \tilde{\mathbf{F}}^H \mathbf{G}_k^H \\ &+ \sigma_{G_k}^2 tr\Big(\tilde{\mathbf{F}}\big(\mathbf{Z}_k' + \sigma_{H_k,\tau}^2 tr(\mathbf{V}_{k,\tau} \mathbf{V}_{k,\tau}^H)\mathbf{I}\big)\tilde{\mathbf{F}}^H\Big) \Big]^{-1} \\ &\times \mathbf{G}_k \tilde{\mathbf{F}} \mathbf{H}_{k,\tau} \mathbf{V}_{k,\tau}. \end{aligned} \tag{38}$$

We use the similar iterative approach as given in Table. 1 to compute the optimal matrices. Further, we employ the OMP algorithm as discussed in Sec. IV in order to obtain the hybrid processors to achieve reduced hardware complexity.

VI. SIMULATION RESULTS

In this section, we present the performance evaluation of the proposed designs via simulation experiments. The performance is evaluated in terms of SMSE and sum-rate (ϖ) versus signal-to-noise-ratio (SNR). The sum-rate is evaluated as $\varpi = \sum_{k=1}^{2} \log_2\big(\det(\mathbf{I}_{N_s} + \varsigma_k)\big)$ bits/sec/Hz, where $\varsigma_k = \frac{\mathbf{R}_k^H \mathbf{G}_k \mathbf{F} \mathbf{H}_k \mathbf{V}_k \mathbf{V}_k^H \mathbf{H}_k^H \mathbf{F}^H \mathbf{G}_k^H \mathbf{R}_k}{\mathbf{R}_k^H \Xi_k \mathbf{R}_k}$ with $\Xi_k = \alpha^{-2}(\sigma_{n_r}^2 \mathbf{I} + \sigma_e^2 \mathbf{I}) + \sigma_n^2 \mathbf{G}_k \mathbf{F}(\mathbf{I} + \mathbf{\Psi})\mathbf{F}^H \mathbf{G}_k^H$. We compare the performance of following schemes:

1) proposed hybrid scheme assuming perfect CSI (referred to as NR-HY),
2) proposed robust hybrid scheme with imperfect CSI (R-HY),
3) fully-digital scheme assuming perfect CSI (NR-FC),
4) robust fully-digital scheme with imperfect CSI (R-FC).

We consider that the distance between the relay and each user is 100 meters and the carrier frequency is 28 GHz. The number of RF chains associated with each user at both the transmitter and receiver unit is set as $\overline{N}_t \geq 2N_s$ with $N_s = 2$. All the simulations are conducted for 10 consecutive time slots while considering the effect of residual LSI accumulated from all previous time slots. For simplicity, in each time slot, all the nodes are assumed to transmit with power $P_1 = P_2 = P_T = P = 0.5$ W. The noise variance at all the receiving nodes is set to $\sigma_{n_1}^2 = \sigma_{n_2}^2 = \sigma_{n_r}^2 = \sigma_n^2 = P/SNR$ and the variance of the loopback channel estimation errors is set to $\sigma_{e_1}^2 = \sigma_{e_2}^2 = \sigma_{e_r}^2 = \sigma_l^2 = INR\sigma_n^2$, where INR is interference-to-noise-ratio. In order to incorporate the robustness in the system design, we consider the channel estimation errors variance to be $\sigma_{H_1}^2 = \sigma_{H_2}^2 = \sigma_{G_1}^2 = \sigma_{G_2}^2 = \sigma_e^2$. The channel follows Saleh-Valenzuela model with uniform linear antenna arrays having inter-element spacing as $\lambda/2$. The number of clusters and number of rays are assumed to be $N_{cl} = 4$ and $N_{ray} = 5$, respectively. BPSK modulation scheme is assumed for generation of data. All the simulations parameters have been tested for $N = 10000$ data samples. The convergence threshold Λ considered for iterative algorithm in Table. 1 is 10^{-4}.

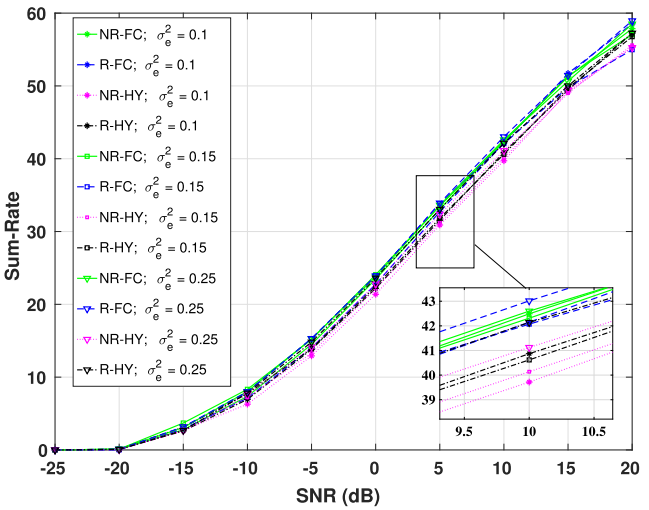

FIGURE 2. Sum-rate Vs SNR performance comparing schemes 1) to 4) for varying error variance.

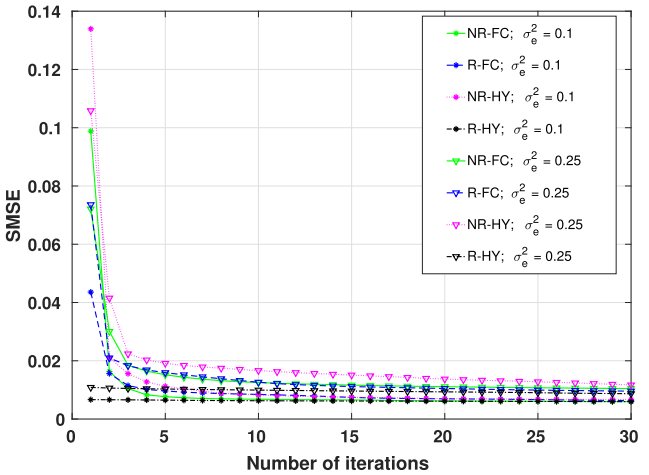

FIGURE 3. Convergence behavior of schemes 1) to 4) with varying error variance for INR = −5dB.

The sum-rate performance with varying SNR values for the proposed FD system with reduced complexity and a FD fully-digital system for both robust and non-robust schemes is compared in Fig. 2 for $N_t = 8$, $N_{rel} = 16$, $\overline{N}_t = 4$, $\overline{N}_{rel} = 8$, $\sigma_e^2 = 0.2$ and INR $= -5$dB. We can observe robustness of the proposed robust design in terms of sum-rate values for different CSI error variances as compared to other designs. Moreover, it is seen that sum-rate comparable to the fully-digital system is achieved with half hardware complexity. Fig. 3 and Fig. 4 show the convergence

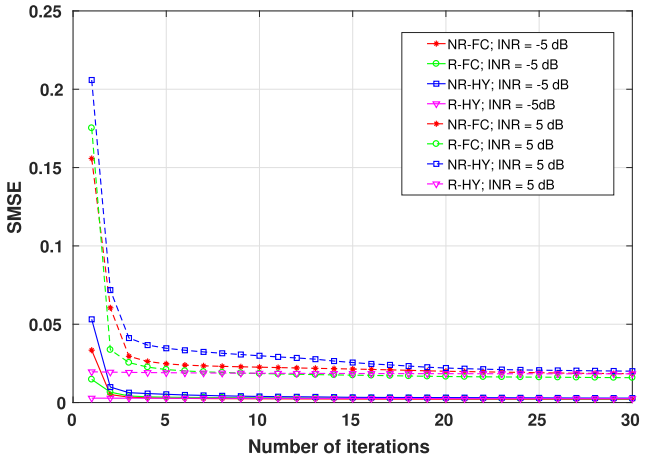

FIGURE 4. Convergence behavior of schemes 1) to 4) with varying INR for $\sigma_e^2 = 0.2$.

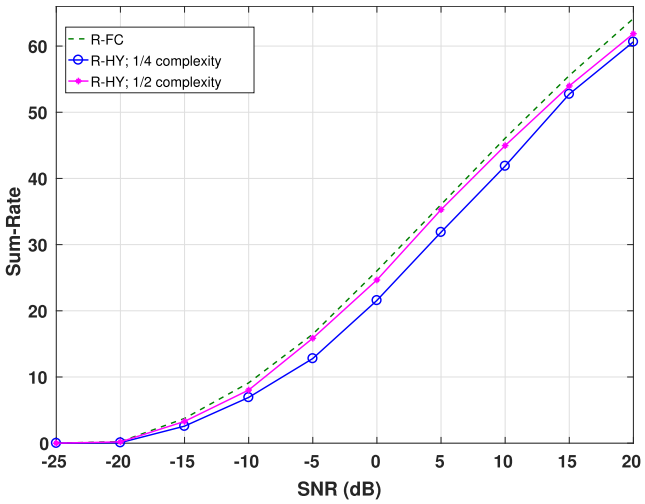

FIGURE 5. Sum-rate Vs SNR performance for varying hardware complexity.

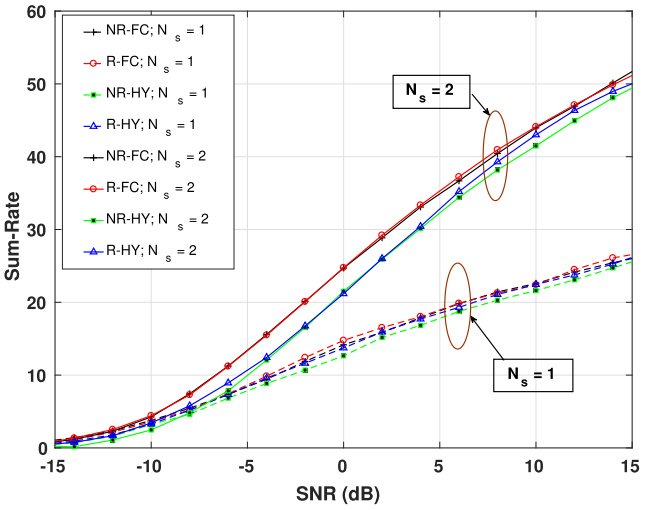

FIGURE 6. Sum-rate Vs SNR performance for varying number of parallel data streams.

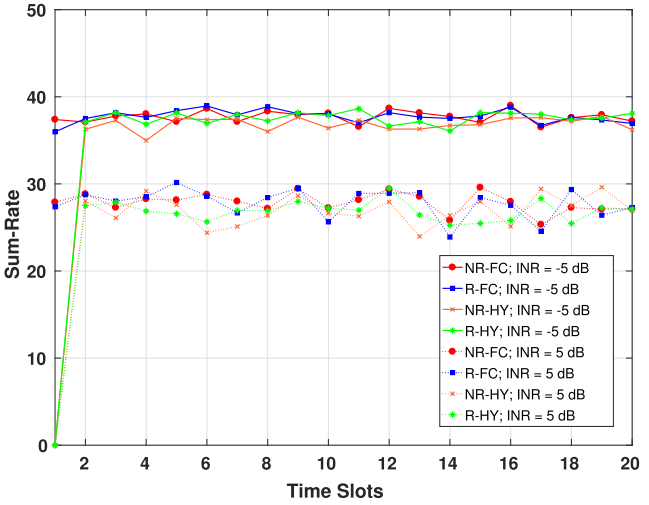

FIGURE 7. Evolution of sum-rate over time for schemes 1) to 4) with varying *INR*.

behavior of the proposed iterative approach with respect to error variance σ_e^2 and INR values, respectively, for $N_t = 8$, $N_{rel} = 16$, $\overline{N}_t = 4$, and $\overline{N}_{rel} = 8$. It is observed that for each time slot, the proposed algorithm converges in less than 5 iterations for all the schemes. By setting $N_t = 16$, $N_{rel} = 32$, $\sigma_e^2 = 0.2$ and $INR = -5$dB, we further examine the effect of varying hardware complexity on the proposed robust designs and the results are shown in Fig. 5. It is observed that comparable sum-rate is obtained with half the hardware complexity of the fully-digital system whereas we observe marginal difference in sum-rate at 1/4 complexity. This implies the proposed design is amenable to implementation in large-MIMO mmWave systems. The detailed analysis of system performance with varying hardware complexity is provided in Sec. VI-A. We also evaluate the sum-rate performance for both the proposed system designs based on varying number of parallel data streams N_s as shown in Fig. 6 for $N_t = 8$, $N_{rel} = 16$, $\overline{N}_t = 4$, $\overline{N}_{rel} = 8$, $\sigma_e^2 = 0.2$, and INR $= -5$dB. As expected, higher sum-rate is achieved with increasing number of data streams as more data can be communicated at each time slot. However, we observe that comparable sum-rate is achieved for all N_s values at lower *SNR* ranges due to insufficient signal strength to carry out multi-stream data transmission. We again set $N_t = 8$, $N_{rel} = 16$, $\overline{N}_t = 4$, $\overline{N}_{rel} = 8$, $\sigma_e^2 = 0.2$ in Fig. 7, which depicts the sum-rate variation in the proposed systems over the time slots for varying INR values. We observe that the sum-rate is distributed with very small standard deviation and constant mean. Also, lower INR values are observed to perform better due to less interference in the system. SMSE and sum-rate plots are shown in Fig. 8 and 9 respectively, considering various dictionaries including eigen beamforming, discrete Fourier transform (DFT) beamforming, discrete cosine transform (DCT) beamforming, discrete Hadamard transform (DHT) beamforming, and antenna selection for

TABLE 4. Hardware complexity analysis.

Hardware Complexity	Sum-rate (bits/sec/Hz)		%SRA	
	Perfect CSI	Imperfect CSI	Perfect CSI	Imperfect CSI
100%(Fully-digital)	25.340	26.749	/	/
50%	23.981	25.757	94.46	96.30
25%	21.156	23.0024	83.48	86.00

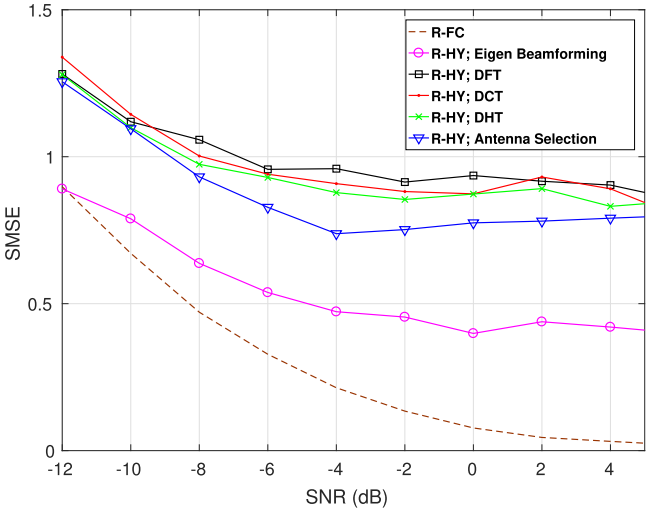

FIGURE 8. SMSE Vs SNR performance for different dictionaries.

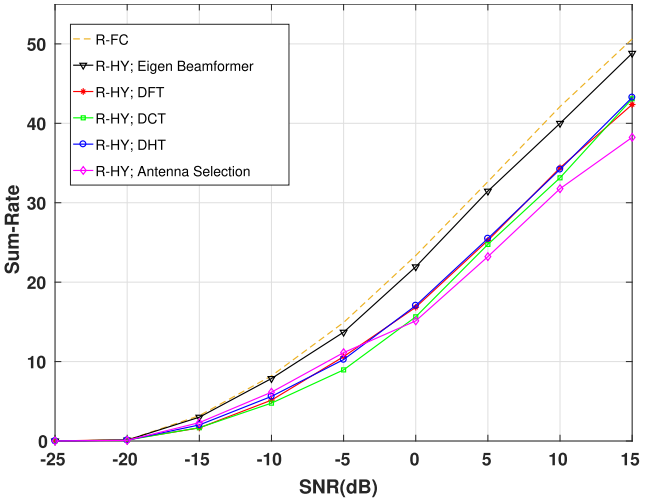

FIGURE 9. Sum-rate Vs SNR performance for various dictionaries.

$N_t = 16$, $N_{rel} = 32$, $\overline{N}_t = 8$, $\overline{N}_{rel} = 16$, $\sigma_e^2 = 0.2$ and INR $= -5$dB. In Fig. 8, we find that SMSE decreases with increasing SNR for all the dictionaries with eigen beamformer performing closest to the fully-digital system. For all other dictionaries, we get higher SMSE values over the entire range of SNR. Similar trend is manifest in Fig. 9 as well. In practical system implementation, the choice of dictionaries will be dictated by application and ease of implementation.

A. HARDWARE COMPLEXITY ANALYSIS

In this subsection, we present the analysis of system performance with varying hardware complexity by using the data collected through extensive simulations. By hardware complexity we refer to the number of RF chains associated with total number of antennas at each user and relay node. We compare both the proposed designs at $1/2$ and $1/4$ hardware complexity against fully-digital system. Sum-rate accuracy ($\%SRA$) is considered as the performance criterion for comparison where $\%SRA$ is computed as $\%SRA = (\varpi_{HY}/\varpi_{FC}) * 100$. We consider sum-rate averaged in SNR range of -10dB to 10dB over 1000 simulations for SRA computation. All the simulations are performed for $N_t = 16$, $N_{rel} = 24$ with associated RF chains $\bar{N}_t \in \{16, 8, 4\}$ and $\bar{N}_{rel} \in \{24, 12, 6\}$ for fully-digital, $1/2$, and $1/4$ hardware complexity, respectively. Complete analysis results are given in Table 4. It is found that the system is able to achieve up to 94 $\%SRA$ with half the complexity and up to 83 $\%SRA$ when hardware complexity reduces to $1/4$ of the fully-digital system. Hence, comparable system performance can be achieved with half the cost as compared to full-complexity systems. Also, $1/4$ complex system have considerable performance with very low cost. Such systems can be considered when low cost communication is a requirement with observed trade-off over the performance. Moreover, it is also seen that the robust system achieves better performance as compared to the system designed by considering perfect CSI knowledge, hence demonstrating its resilience towards CSI errors even with reduced hardware complexity.

VII. CONCLUSION

In this paper, we investigated low-complexity hybrid FD relay-based mmWave communication systems. We proposed transceiver and relay filter designs for the case where the available CSI of all the links except the loopback channels are perfectly known as well as the case where the CSI of all the links are imperfect. The hybrid RF/baseband architecture was considered in order to achieve reduction in hardware complexity and hence making it feasible for implementation in mmWave systems employing large number of antenna elements. For both the designs, we first jointly obtained the full-complexity optimal transceiver and relay filter matrices under the total relay transmit power constraint using an iterative approach. A closed form solution for relay-filter at each time slot, was obtained by minimizing the SMSE while reducing the effect of residual LSI. We further

decomposed the optimal filters into analog-digital hybrid matrices by using an OMP-based sparse approximation technique. We illustrated through simulations that both the proposed hybrid designs with reduced hardware complexities are capable of performance comparable to the full-complexity fully-digital system. Furthermore, in the proposed robust design, we considered the imperfections in channel knowledge while designing the overall system making the performance resilient to CSI errors. We also validated the robustness of the proposed design in the presence of CSI errors through simulations.

APPENDIX A
OPTIMIZATION PROBLEM SOLUTION

In this section, we present the generalized solution of the optimization problem given in (13) and (34) for both the proposed designs by using Karush-Kuhn-Tucker conditions. We introduce an additional term χ in the expressions to differentiate between both the proposed designs. We consider $\chi = 1$ for the robust system and $\chi = 0$ otherwise. The generalized Lagrangian function $J(\alpha, \mathbf{V}_{1,\tau}, \mathbf{V}_{2,\tau}, \mathbf{R}_1, \mathbf{R}_2, \tilde{\mathbf{F}}, \lambda)$ associated with the optimization problem is given by

$$\begin{aligned}
&J(\alpha, \mathbf{V}_{1,\tau}, \mathbf{V}_{2,\tau}, \mathbf{R}_1, \mathbf{R}_2, \tilde{\mathbf{F}}, \lambda)\\
&= N_s(P_1+P_2) - \mathrm{tr}(\mathbf{R}_2^H \mathbf{G}_2 \tilde{\mathbf{F}} \mathbf{H}_{1,\tau} \mathbf{V}_{1,\tau}\\
&\quad + \mathbf{V}_{1,\tau}^H \mathbf{H}_{1,\tau}^H \tilde{\mathbf{F}}^H \mathbf{G}_2^H \mathbf{R}_2 + \mathbf{R}_1^H \mathbf{G}_1 \tilde{\mathbf{F}} \mathbf{H}_{2,\tau} \mathbf{V}_{2,\tau}\\
&\quad + \mathbf{V}_{2,\tau}^H \mathbf{H}_{2,\tau}^H \tilde{\mathbf{F}}^H \mathbf{G}_1^H \mathbf{R}_1) + \alpha^{-2}\big(\sigma_{n_1}^2\\
&\quad + \sigma_{e_1}^2 \mathrm{tr}(\mathbf{V}_1 \mathbf{V}_1^H)\big)\mathrm{tr}(\mathbf{R}_1 \mathbf{R}_1^H) + \alpha^{-2}\big(\sigma_{n_2}^2\\
&\quad + \sigma_{e_2}^2 \mathrm{tr}(\mathbf{V}_2 \mathbf{V}_2^H)\big)\mathrm{tr}(\mathbf{R}_2 \mathbf{R}_2^H)\\
&\quad + \mathrm{tr}(\mathbf{R}_1^H \mathbf{G}_1 \tilde{\mathbf{F}} \mathbf{Z}_1^\chi \tilde{\mathbf{F}}^H \mathbf{G}_1^H \mathbf{R}_1) + \chi \sigma_{G_1}^2 \mathrm{tr}\Big(\tilde{\mathbf{F}}\big(\mathbf{Z}_1^\chi\\
&\quad + \sigma_{H_2,\tau}^2 \mathrm{tr}(\mathbf{V}_{2,\tau} \mathbf{V}_{2,\tau}^H)\mathbf{I}\big)\tilde{\mathbf{F}}^H\Big)\mathrm{tr}(\mathbf{R}_1 \mathbf{R}_1^H)\\
&\quad + \mathrm{tr}(\mathbf{R}_2^H \mathbf{G}_2 \tilde{\mathbf{F}} \mathbf{Z}_2^\chi \tilde{\mathbf{F}}^H \mathbf{G}_2^H \mathbf{R}_2)\\
&\quad + \chi \sigma_{G_2}^2 \mathrm{tr}\Big(\tilde{\mathbf{F}}\big(\mathbf{Z}_2^\chi + \sigma_{H_1,\tau}^2 \mathrm{tr}(\mathbf{V}_{1,\tau} \mathbf{V}_{1,\tau}^H)\mathbf{I}\big)\tilde{\mathbf{F}}^H\Big)\mathrm{tr}(\mathbf{R}_2 \mathbf{R}_2^H)\\
&\quad + \lambda\big(\alpha^2 \mathrm{tr}(\tilde{\mathbf{F}} \mathbf{Z}_r^\chi \tilde{\mathbf{F}}^H) - P_T\big), \qquad (39)
\end{aligned}$$

where,

$$\mathbf{Z}_i^\chi = \begin{cases} \mathbf{Z}_i, & \chi = 0 \\ \mathbf{Z}_i', & \chi = 1 \end{cases} \quad \forall i \in \{1, 2, r\} \qquad (40)$$

We obtain the desired transceiver and relay filter matrices by minimization with respect to each dependent variable in the Lagrangian. Differentiating the Lagrangian w.r.t. $\mathbf{V}_{1,\tau}^H$ and setting it to zero, we have

$$\begin{aligned}
\frac{\partial J}{\partial \mathbf{V}_{1,\tau}^H} &= -\mathbf{H}_{1,\tau}^H \tilde{\mathbf{F}}^H \mathbf{G}_2^H \mathbf{R}_2 + \mathbf{H}_{1,\tau}^H \tilde{\mathbf{F}}^H \mathbf{G}_2^H \mathbf{R}_2 \mathbf{R}_2^H \mathbf{G}_2 \tilde{\mathbf{F}} \mathbf{H}_{1,\tau} \mathbf{V}_{1,\tau}\\
&\quad + \chi \sigma_{H_1,\tau}^2 \sigma_{G_2}^2 \mathrm{tr}(\tilde{\mathbf{F}}^H \tilde{\mathbf{F}}) \mathrm{tr}(\mathbf{R}_2 \mathbf{R}_2^H) \mathbf{V}_{1,\tau}\\
&\quad + \chi \sigma_{G_2}^2 \mathrm{tr}(\mathbf{R}_2 \mathbf{R}_2^H) \mathbf{H}_{1,\tau}^H \tilde{\mathbf{F}}^H \tilde{\mathbf{F}} \mathbf{H}_{1,\tau} \mathbf{V}_{1,\tau}\\
&\quad + \lambda \alpha^2 \big(\mathbf{H}_{1,\tau}^H \tilde{\mathbf{F}}^H \tilde{\mathbf{F}} \mathbf{H}_{1,\tau} \mathbf{V}_{1,\tau}\\
&\quad + \chi \sigma_{H_1,\tau}^2 \mathrm{tr}(\tilde{\mathbf{F}}^H \tilde{\mathbf{F}}) \mathbf{V}_{1,\tau}\big) = 0,
\end{aligned}$$

From the above, we get the precoder matrix for $U1$ as

$$\begin{aligned}
\mathbf{V}_{1,\tau} &= \Big[\mathbf{H}_{1,\tau}^H \tilde{\mathbf{F}}^H \mathbf{G}_2^H \mathbf{R}_2 \mathbf{R}_2^H \mathbf{G}_2 \tilde{\mathbf{F}} \mathbf{H}_{1,\tau}\\
&\quad + \chi \sigma_{H_1,\tau}^2 \sigma_{G_2}^2 \mathrm{tr}(\tilde{\mathbf{F}}^H \tilde{\mathbf{F}}) \mathrm{tr}(\mathbf{R}_2 \mathbf{R}_2^H) \mathbf{I}\\
&\quad + \chi \sigma_{G_2}^2 \mathrm{tr}(\mathbf{R}_2 \mathbf{R}_2^H) \mathbf{H}_{1,\tau}^H \tilde{\mathbf{F}}^H \tilde{\mathbf{F}} \mathbf{H}_{1,\tau}\\
&\quad + \lambda \alpha^2 \big(\mathbf{H}_{1,\tau}^H \tilde{\mathbf{F}}^H \tilde{\mathbf{F}} \mathbf{H}_{1,\tau}\\
&\quad + \chi \sigma_{H_1,\tau}^2 \mathrm{tr}(\tilde{\mathbf{F}}^H \tilde{\mathbf{F}}) \mathbf{I}\big)\Big]^{-1} \mathbf{H}_{1,\tau}^H \tilde{\mathbf{F}}^H \mathbf{G}_2^H \mathbf{R}_2. \qquad (41)
\end{aligned}$$

Similarly for $U2$, the precoder matrix is obtained as

$$\begin{aligned}
\mathbf{V}_{2,\tau} &= \Big[\mathbf{H}_{2,\tau}^H \tilde{\mathbf{F}}^H \mathbf{G}_1^H \mathbf{R}_1 \mathbf{R}_1^H \mathbf{G}_1 \tilde{\mathbf{F}} \mathbf{H}_{2,\tau}\\
&\quad + \chi \sigma_{H_2,\tau}^2 \sigma_{G_1}^2 \mathrm{tr}(\tilde{\mathbf{F}}^H \tilde{\mathbf{F}}) \mathrm{tr}(\mathbf{R}_1 \mathbf{R}_1^H) \mathbf{I}\\
&\quad + \chi \sigma_{G_1}^2 \mathrm{tr}(\mathbf{R}_1 \mathbf{R}_1^H) \mathbf{H}_{2,\tau}^H \tilde{\mathbf{F}}^H \tilde{\mathbf{F}} \mathbf{H}_{2,\tau}\\
&\quad + \lambda \alpha^2 \big(\mathbf{H}_{2,\tau}^H \tilde{\mathbf{F}}^H \tilde{\mathbf{F}} \mathbf{H}_{2,\tau}\\
&\quad + \chi \sigma_{H_2,\tau}^2 \mathrm{tr}(\tilde{\mathbf{F}}^H \tilde{\mathbf{F}}) \mathbf{I}\big)\Big]^{-1} \mathbf{H}_{2,\tau}^H \tilde{\mathbf{F}}^H \mathbf{G}_1^H \mathbf{R}_1. \qquad (42)
\end{aligned}$$

Now, differentiating the Lagrangian w.r.t. $\mathbf{R}_1^H$ and setting it to zero, we get

$$\begin{aligned}
\frac{\partial J}{\partial \mathbf{R}_1^H} &= -\mathbf{G}_1 \tilde{\mathbf{F}} \mathbf{H}_{2,\tau} \mathbf{V}_{2,\tau} + \alpha^{-2}\big(\sigma_{n_1}^2 + \sigma_{e_1}^2 \mathrm{tr}(\mathbf{V}_1 \mathbf{V}_1^H)\big)\mathbf{R}_1\\
&\quad + \mathbf{G}_1 \tilde{\mathbf{F}} \mathbf{Z}_1^\chi \tilde{\mathbf{F}}^H \mathbf{G}_1^H \mathbf{R}_1 + \chi \sigma_{G_1}^2 \mathrm{tr}\Big(\tilde{\mathbf{F}}\big(\mathbf{Z}_1^\chi\\
&\quad + \sigma_{H_2,\tau}^2 \mathrm{tr}(\mathbf{V}_{2,\tau} \mathbf{V}_{2,\tau}^H)\mathbf{I}\big)\tilde{\mathbf{F}}^H \mathbf{R}_1\Big) = 0.
\end{aligned}$$

Thus the receive filter for $U1$ is obtained as

$$\begin{aligned}
\mathbf{R}_1 &= \Big[\alpha^{-2}\big(\sigma_{n_1}^2 + \sigma_{e_1}^2 \mathrm{tr}\big(\mathbf{V}_1 \mathbf{V}_1^H\big)\big)\mathbf{I} + \mathbf{G}_1 \tilde{\mathbf{F}} \mathbf{Z}_1^\chi \tilde{\mathbf{F}}^H \mathbf{G}_1^H\\
&\quad + \chi \sigma_{G_1}^2 \mathrm{tr}\Big(\tilde{\mathbf{F}}\big(\mathbf{Z}_1^\chi + \sigma_{H_2,\tau}^2 \mathrm{tr}(\mathbf{V}_{2,\tau} \mathbf{V}_{2,\tau}^H)\mathbf{I}\big)\tilde{\mathbf{F}}^H\Big)\Big]^{-1}\\
&\quad \times \mathbf{G}_1 \tilde{\mathbf{F}} \mathbf{H}_{2,\tau} \mathbf{V}_{2,\tau}. \qquad (43)
\end{aligned}$$

Similarly, the receive filter for $U2$ is given as

$$\begin{aligned}
\mathbf{R}_2 &= \Big[\alpha^{-2}\big(\sigma_{n_2}^2 + \sigma_{e_2}^2 \mathrm{tr}(\mathbf{V}_2 \mathbf{V}_2^H)\big)\mathbf{I} + \mathbf{G}_2 \tilde{\mathbf{F}} \mathbf{Z}_2^\chi \tilde{\mathbf{F}}^H \mathbf{G}_2^H\\
&\quad + \chi \sigma_{G_2}^2 \mathrm{tr}\Big(\tilde{\mathbf{F}}\big(\mathbf{Z}_2^\chi + \sigma_{H_1,\tau}^2 \mathrm{tr}(\mathbf{V}_{1,\tau} \mathbf{V}_{1,\tau}^H)\mathbf{I}\big)\tilde{\mathbf{F}}^H\Big)\Big]^{-1}\\
&\quad \times \mathbf{G}_2 \tilde{\mathbf{F}} \mathbf{H}_{1,\tau} \mathbf{V}_{1,\tau}. \qquad (44)
\end{aligned}$$

In order to obtain the expression for relay filter, we differentiate the Lagrangian w.r.t. $\tilde{\mathbf{F}}^H$ and obtain

$$\begin{aligned}
\frac{\partial J}{\partial \tilde{\mathbf{F}}^H} &= -(\mathbf{G}_2^H \mathbf{R}_2 \mathbf{V}_{1,\tau}^H \mathbf{H}_{1,\tau}^H + \mathbf{G}_1^H \mathbf{R}_1 \mathbf{V}_{2,\tau}^H \mathbf{H}_{2,\tau}^H)\\
&\quad + (\mathbf{G}_1^H \mathbf{R}_1 \mathbf{R}_1^H \mathbf{G}_1^H) \tilde{\mathbf{F}} \mathbf{Z}_1^\chi + (\mathbf{G}_2^H \mathbf{R}_2 \mathbf{R}_2^H \mathbf{G}_2^H) \tilde{\mathbf{F}} \mathbf{Z}_2^\chi\\
&\quad + \chi \Big(\sigma_{G_1}^2 \big(\mathrm{tr}(\mathbf{R}_1 \mathbf{R}_1^H)\mathbf{I}\big)\tilde{\mathbf{F}}\big(\mathbf{Z}_1^\chi + \sigma_{H_2,\tau}^2 \mathrm{tr}(\mathbf{V}_2 \mathbf{V}_2^H)\mathbf{I}\big)\Big)\\
&\quad + \chi \Big(\sigma_{G_2}^2 \big(\mathrm{tr}(\mathbf{R}_2 \mathbf{R}_2^H)\mathbf{I}\big)\tilde{\mathbf{F}}\big(\mathbf{Z}_2^\chi + \sigma_{H_1,\tau}^2 \mathrm{tr}(\mathbf{V}_1 \mathbf{V}_1^H)\mathbf{I}\big)\Big)\\
&\quad + \lambda \alpha^2 \tilde{\mathbf{F}} \mathbf{Z}_r^\chi = 0. \qquad (45)
\end{aligned}$$

For simplicity, we denote

$$\begin{aligned}\mathbf{B} &= \mathbf{G}_2^H\mathbf{R}_2\mathbf{V}_{1,\tau}^H\mathbf{H}_{1,\tau}^H + \mathbf{G}_1^H\mathbf{R}_1\mathbf{V}_{2,\tau}^H\mathbf{H}_{2,\tau}^H,\\ \mathbf{D}_I &= \mathbf{G}_1^H\mathbf{R}_1\mathbf{R}_1^H\mathbf{G}_1^H,\\ \mathbf{D}_{II} &= \mathbf{G}_2^H\mathbf{R}_2\mathbf{R}_2^H\mathbf{G}_2^H,\\ \mathbf{D}_{III} &= \mathbf{Z}_1^{\chi} + \sigma_{H_2,\tau}^2 tr(\mathbf{V}_2\mathbf{V}_2^H)\mathbf{I}, \quad \text{and,}\\ \mathbf{D}_{IV} &= \mathbf{Z}_2^{\chi} + \sigma_{H_1,\tau}^2 tr(\mathbf{V}_1\mathbf{V}_1^H)\mathbf{I}.\end{aligned}$$

Hence, the expression in (45) can be rewritten as

$$\begin{aligned}\frac{\partial J}{\partial \tilde{\mathbf{F}}^H} &= -\mathbf{B} + \mathbf{D}_I\tilde{\mathbf{F}}\mathbf{Z}_1^{\chi} + \mathbf{D}_{II}\tilde{\mathbf{F}}\mathbf{Z}_2^{\chi}\\ &\quad + \chi\left(\sigma_{G_1}^2\left(tr(\mathbf{R}_1\mathbf{R}_1^H)\mathbf{I}\right)\tilde{\mathbf{F}}\mathbf{D}_{III}\right)\\ &\quad + \chi\left(\sigma_{G_2}^2\left(tr(\mathbf{R}_2\mathbf{R}_2^H)\mathbf{I}\right)\tilde{\mathbf{F}}\mathbf{D}_{IV}\right)\\ &\quad + \lambda\alpha^2\tilde{\mathbf{F}}\mathbf{Z}_r^{\chi} = 0\\ \Longrightarrow\ & \mathbf{D}_I\tilde{\mathbf{F}}\mathbf{Z}_1^{\chi} + \mathbf{D}_{II}\tilde{\mathbf{F}}\mathbf{Z}_2^{\chi} + \chi\left(\sigma_{G_1}^2\left(tr(\mathbf{R}_1\mathbf{R}_1^H)\mathbf{I}\right)\tilde{\mathbf{F}}\mathbf{D}_{III}\right)\\ &\quad + \chi\left(\sigma_{G_2}^2\left(tr(\mathbf{R}_2\mathbf{R}_2^H)\mathbf{I}\right)\tilde{\mathbf{F}}\mathbf{D}_{IV}\right) + \lambda\alpha^2\tilde{\mathbf{F}}\mathbf{Z}_r^{\chi} = \mathbf{B}.\end{aligned}$$

On performing the vectorization operation on the preceding equation, we get

$$\begin{aligned}vec\Big(&\mathbf{D}_I\tilde{\mathbf{F}}\mathbf{Z}_1^{\chi} + \mathbf{D}_{II}\tilde{\mathbf{F}}\mathbf{Z}_2^{\chi} + \chi\left(\sigma_{G_1}^2\left(tr(\mathbf{R}_1\mathbf{R}_1^H)\mathbf{I}\right)\tilde{\mathbf{F}}\mathbf{D}_{III}\right)\\ &+ \chi\left(\sigma_{G_2}^2\left(tr(\mathbf{R}_2\mathbf{R}_2^H)\mathbf{I}\right)\tilde{\mathbf{F}}\mathbf{D}_{IV}\right) + \lambda\alpha^2\tilde{\mathbf{F}}\mathbf{Z}_r^{\chi}\Big) = vec(\mathbf{B}).\end{aligned}$$

For any three matrices, $\mathbf{A}_1$, $\mathbf{A}_2$, and $\mathbf{A}_3$ of suitable dimensions, $vec(\mathbf{A}_1\mathbf{A}_2\mathbf{A}_3) = (\mathbf{A}_3{}^T \otimes \mathbf{A}_1)vec(\mathbf{A}_2)$, [46]. Thus, we have

$$\widehat{\mathbf{f}} = \mathbf{O}^{-1}\mathbf{f},$$

where, $\widehat{\mathbf{f}} = vec(\tilde{\mathbf{F}})$, $\mathbf{f} = vec(\mathbf{B})$ and $\mathbf{O} = (\mathbf{Z}_1^{\chi T} \otimes \mathbf{D}_I) + (\mathbf{Z}_2^{\chi T} \otimes \mathbf{D}_{II}) + \chi\left(\mathbf{D}_{III}^T \otimes \sigma_{G_1}^2\left(tr(\mathbf{R}_1\mathbf{R}_1^H)\mathbf{I}\right)\right) + \chi\left(\mathbf{D}_{IV}^T \otimes \sigma_{G_2}^2\left(tr(\mathbf{R}_2\mathbf{R}_2^H)\mathbf{I}\right)\right) + (\mathbf{Z}_r^{\chi T} \otimes \lambda\alpha^2\mathbf{I})$. Hence, the relay filter matrix $\mathbf{F}$ can be obtained as

$$\mathbf{F} = \alpha\tilde{\mathbf{F}}. \tag{46}$$

Differentiating the Lagrangian w.r.t α, we have

$$\begin{aligned}\frac{\partial J}{\partial \alpha} &= -2\alpha^{-3}\left(\sigma_{n_1}^2 + \sigma_{e_1}^2 tr(\mathbf{V}_1\mathbf{V}_1^H)\right)tr(\mathbf{R}_1\mathbf{R}_1^H)\\ &\quad - 2\alpha^{-3}(\sigma_{n_2}^2 + \sigma_{e_2}^2 tr\left(\mathbf{V}_2\mathbf{V}_2^H\right))tr(\mathbf{R}_2\mathbf{R}_2^H)\\ &\quad + \lambda\left(2\alpha tr(\tilde{\mathbf{F}}\mathbf{Z}_r^{\chi}\tilde{\mathbf{F}}^H)\right),\end{aligned}$$

and setting it to zero, we get

$$\begin{aligned}\alpha\lambda tr(\tilde{\mathbf{F}}\mathbf{Z}_r^{\chi}\tilde{\mathbf{F}}^H) &= \alpha^{-3}\sum_{i=1}^{2}(\sigma_{n_i}^2 + \sigma_{e_i}^2 tr(\mathbf{V}_i\mathbf{V}_i^H))tr(\mathbf{R}_i\mathbf{R}_i^H),\\ &\Rightarrow \alpha^2 tr(\tilde{\mathbf{F}}\mathbf{Z}_r^{\chi}\tilde{\mathbf{F}}^H)\\ &= \frac{\alpha^{-2}\sum_{i=1}^{2}\left(\sigma_{n_i}^2 + \sigma_{e_i}^2 tr(\mathbf{V}_i\mathbf{V}_i^H)\right)tr(\mathbf{R}_i\mathbf{R}_i^H)}{\lambda}.\end{aligned} \tag{47}$$

Finally differentiating the Lagrangian w.r.t λ and equating it to zero we get

$$\begin{aligned}\frac{\partial J}{\partial \lambda} &= \alpha^2 tr(\tilde{\mathbf{F}}\mathbf{Z}_r^{\chi}\tilde{\mathbf{F}}^H) - P_T = 0.\\ &\Rightarrow \alpha^2 tr(\tilde{\mathbf{F}}\mathbf{Z}_r^{\chi}\tilde{\mathbf{F}}^H) = P_T,\\ &\Rightarrow \frac{\alpha^{-2}\sum_{i=1}^{2}\left(\sigma_{n_i}^2 + \sigma_{e_i}^2 tr(\mathbf{V}_i\mathbf{V}_i^H)\right)tr(\mathbf{R}_i\mathbf{R}_i^H)}{\lambda} = P_T,\\ &\Rightarrow \lambda\alpha^2 = \frac{\sum_{i=1}^{2}\left(\sigma_{n_i}^2 + \sigma_{e_i}^2 tr(\mathbf{V}_i\mathbf{V}_i^H)\right)tr(\mathbf{R}_i\mathbf{R}_i^H)}{P_T}.\end{aligned} \tag{48}$$

Hence, α can be calculated as

$$\alpha = \sqrt{N_{rel}P_T\left(tr(\tilde{\mathbf{F}}\mathbf{Z}_r^{\chi}\tilde{\mathbf{F}}^H)\right)^{-1}}, \tag{49}$$

and λ is obtained as

$$\begin{aligned}\lambda = (N_{rel}P_T)^{-2}\Big(&\sum_{i=1}^{2}\left(\sigma_{n_i}^2 + \sigma_{e_i}^2 tr(\mathbf{V}_i\mathbf{V}_i^H)\right)tr(\mathbf{R}_i\mathbf{R}_i^H)\Big)\\ &\times tr(\tilde{\mathbf{F}}\mathbf{Z}_r^{\chi}\tilde{\mathbf{F}}^H).\end{aligned} \tag{50}$$

REFERENCES

[1] Z. Pi and F. Khan, "An introduction to millimeter-wave mobile broadband systems," *IEEE Commun. Mag.*, vol. 49, no. 6, pp. 101–107, Jun. 2011.
[2] T. S. Rappaport *et al.*, "Millimeter wave mobile communications for 5G cellular: It will work!" *IEEE Access*, vol. 1, pp. 335–349, May 2013.
[3] M. Xiao *et al.*, "Millimeter wave communications for future mobile networks," *IEEE J. Sel. Areas Commun.*, vol. 35, no. 9, pp. 1909–1935, Sep. 2017.
[4] S. K. Yong and C.-C. Chong, "An overview of multigigabit wireless through millimeter wave technology: Potentials and technical challenges," *EURASIP J. Wireless Commun. Netw.*, vol. 2007, no. 1, p. 078907, 2006.
[5] O. El Ayach, S. Rajagopal, S. Abu-Surra, Z. Pi, and R. W. Heath, Jr., "Spatially sparse precoding in millimeter wave MIMO systems," *IEEE Trans. Wireless Commun.*, vol. 13, no. 3, pp. 1499–1513, Mar. 2014.
[6] J. Mao, Z. Gao, Y. Wu, and M.-S. Alouini, "Over-sampling codebook-based hybrid minimum sum-mean-square-error precoding for millimeter-wave 3D-MIMO," *IEEE Wireless Commun. Lett.*, vol. 7, no. 6, pp. 938–941, Dec. 2018.
[7] Y. Sun, Z. Gao, H. Wang, and D. Wu, "Wideband hybrid precoding for next-generation backhaul/fronthaul based on mmWave FD-MIMO," in *Proc. IEEE Global Commun. Conf. Workshops*, to be published. [Online]. Available: http://arxiv.org/abs/1809.03367v1
[8] A. Alkhateeb, O. El Ayach, G. Leus, and R. W. Heath, Jr., "Hybrid precoding for millimeter wave cellular systems with partial channel knowledge," in *Proc. Inf. Theory Appl. Workshop (ITA)*, Feb. 2013, pp. 1–5.
[9] F. Sohrabi and W. Yu, "Hybrid digital and analog beamforming design for large-scale MIMO systems," in *Proc. IEEE Int. Conf. Acoust., Speech Signal Process. (ICASSP)*, Apr. 2015, pp. 2929–2933.
[10] J. Lee and Y. H. Lee, "AF relaying for millimeter wave communication systems with hybrid RF/baseband MIMO processing," in *Proc. IEEE Int. Conf. Commun. (ICC)*, Jun. 2014, pp. 5838–5842.
[11] D. Jagyasi and P. Ubaidulla, "Low-complexity two-way AF relay design for millimeter wave communication systems," in *Proc. IEEE 85th Veh. Technol. Conf. (VTC Spring)*, Jun. 2017, pp. 1–5.
[12] M. Kim and Y. H. Lee, "MSE-based hybrid RF/baseband processing for millimeter-wave communication systems in MIMO interference channels," *IEEE Trans. Veh. Technol.*, vol. 64, no. 6, pp. 2714–2720, Jun. 2015.
[13] F. Sohrabi and W. Yu, "Hybrid analog and digital beamforming for mmWave OFDM large-scale antenna arrays," *IEEE J. Sel. Areas Commun.*, vol. 35, no. 7, pp. 1432–1443, Jul. 2017.
[14] S. Rangan, T. S. Rappaport, and E. Erkip, "Millimeter-wave cellular wireless networks: Potentials and challenges," *Proc. IEEE*, vol. 102, no. 3, pp. 366–385, Mar. 2014.
[15] M. R. Akdeniz *et al.*, "Millimeter wave channel modeling and cellular capacity evaluation," *IEEE J. Sel. Areas Commun.*, vol. 32, no. 6, pp. 1164–1179, Jun. 2014.

[16] B. Ma, H. Shah-Mansouri, and V. W. S. Wong, "Full-duplex relaying for D2D communication in millimeter wave-based 5G networks," *IEEE Trans. Wireless Commun.*, vol. 17, no. 7, pp. 4417–4431, Jul. 2018.
[17] G. Yang, J. Du, and M. Xiao, "Maximum throughput path selection with random blockage for indoor 60 GHz relay networks," *IEEE Trans. Commun.*, vol. 63, no. 10, pp. 3511–3524, Oct. 2015.
[18] J. N. Laneman, D. N. C. Tse, and G. W. Wornell, "Cooperative diversity in wireless networks: Efficient protocols and outage behavior," *IEEE Trans. Inf. Theory*, vol. 50, no. 12, pp. 3062–3080, Dec. 2004.
[19] A. Sendonaris, E. Erkip, and B. Aazhang, "User cooperation diversity. Part I. System description," *IEEE Trans. Commun.*, vol. 51, no. 11, pp. 1927–1938, Nov. 2003.
[20] Y. W. Hong, W. J. Huang, F. H. Chiu, and C. C. J. Kuo, "Cooperative communications in resource-constrained wireless networks," *IEEE Signal Process. Mag.*, vol. 24, no. 3, pp. 47–57, May 2007.
[21] C. L. Wang, J. Y. Chen, and J. J. Jheng, "A precoder design for two-way amplify-and-forward MIMO relay systems with linear receivers," in *Proc. IEEE 80th Veh. Technol. Conf. (VTC Fall)*, Sep. 2014, pp. 1–5.
[22] X. Xue, Y. Wang, X. Wang, and T. E. Bogale, "Joint source and relay precoding in multiantenna millimeter-wave systems," *IEEE Trans. Veh. Technol.*, vol. 66, no. 6, pp. 4924–4937, Jun. 2017.
[23] X. Xue, T. E. Bogale, X. Wang, Y. Wang, and L. B. Le, "Hybrid analog-digital beamforming for multiuser MIMO millimeter wave relay systems," in *Proc. IEEE/CIC Int. Conf. Commun. China (ICCC)*, Nov. 2015, pp. 1–7.
[24] J. S. Sheu, "Hybrid digital and analogue beamforming design for millimeter wave relaying systems," *J. Commun. Netw.*, vol. 19, no. 5, pp. 461–469, Oct. 2017.
[25] G. Liu, F. R. Yu, H. Ji, V. C. M. Leung, and X. Li, "In-band full-duplex relaying for 5G cellular networks with wireless virtualization," *IEEE Netw.*, vol. 29, no. 6, pp. 54–61, Nov. 2015.
[26] G. Liu, F. R. Yu, H. Ji, V. C. M. Leung, and X. Li, "In-band full-duplex relaying: A survey, research issues and challenges," *IEEE Commun. Surveys Tuts.*, vol. 17, no. 2, pp. 500–524, 2nd Quart., 2015.
[27] Z. Wei, X. Zhu, S. Sun, Y. Huang, A. Al-Tahmeesschi, and Y. Jiang, "Energy-efficiency of millimeter-wave full-duplex relaying systems: Challenges and solutions," *IEEE Access*, vol. 4, pp. 4848–4860, Sep. 2016.
[28] H. Abbas and K. Hamdi, "Full duplex relay in millimeter wave backhaul links," in *Proc. IEEE Wireless Commun. Netw. Conf.*, Apr. 2016, pp. 1–6.
[29] H. Krishnaswamy and G. Zussman, "1 chip 2x the bandwidth," *IEEE Spectr.*, vol. 53, no. 7, pp. 38–54, Jul. 2016.
[30] D. Bharadia and S. Katti, "Full duplex MIMO radios," in *Proc. 11th USENIX Symp. Netw. Syst. Design Implement. (NSDI)*, 2014, pp. 359–372.
[31] T. Riihonen, S. Werner, and R. Wichman, "Mitigation of loopback self-interference in full-duplex MIMO relays," *IEEE Trans. Signal Process.*, vol. 59, no. 12, pp. 5983–5993, Dec. 2011.
[32] Z. Xiao, P. Xia, and X.-G. Xia, "Full-duplex millimeter-wave communication," *IEEE Wireless Commun.*, vol. 24, no. 6, pp. 136–143, Dec. 2017.
[33] N. Lee, O. Simeone, and J. Kang, "The effect of imperfect channel knowledge on a MIMO system with interference," *IEEE Trans. Commun.*, vol. 60, no. 8, pp. 2221–2229, Aug. 2012.
[34] P. Ubaidulla and A. Chockalingam, "Relay precoder optimization in MIMO-relay networks with imperfect CSI," *IEEE Trans. Signal Process.*, vol. 59, no. 11, pp. 5473–5484, Nov. 2011.
[35] J. Liu, F. Gao, and Z. Qiu, "Robust transceiver design for downlink multiuser MIMO AF relay systems," *IEEE Trans. Wireless Commun.*, vol. 14, no. 4, pp. 2218–2231, Apr. 2015.
[36] H. Shen, J. Wang, B. Levy, and C. Zhao, "Robust optimization for amplify-and-forward MIMO relaying from a worst-case perspective," *IEEE Trans. Signal Process.*, vol. 61, no. 21, pp. 5458–5471, Nov. 2013.
[37] D. Jagyasi and P. Ubaidulla, "Low-complexity transceiver design for multi-user millimeter wave communication systems under imperfect CSI," in *Proc. IEEE 84th Veh. Technol. Conf. (VTC-Fall)*, Sep. 2016, pp. 1–5.
[38] P. Ubaidulla and A. Chockalingam, "Robust THP transceiver designs for multiuser MIMO downlink," in *Proc. IEEE Wireless Commun. Netw. Conf.*, Apr. 2009, pp. 1–6.
[39] T. Kwon, S. Lim, S. Choi, and D. Hong, "Optimal duplex mode for DF relay in terms of the outage probability," *IEEE Trans. Veh. Technol.*, vol. 59, no. 7, pp. 3628–3634, Sep. 2010.
[40] H. Alves, D. B. da Costa, R. D. Souza, and M. Latva-Aho, "On the performance of two-way half-duplex and one-way full-duplex relaying," in *Proc. IEEE 14th Workshop Signal Process. Adv. Wireless Commun. (SPAWC)*, Jun. 2013, pp. 56–60.
[41] T. S. Rappaport, R. W. Heath, Jr., R. C. Daniels, and J. N. Murdock, *Millimeter Wave Wireless Communications*. London, U.K.: Pearson, 2014.
[42] A. I. Sulyman, A. T. Nassar, M. K. Samimi, G. R. MacCartney, Jr., T. S. Rappaport, and A. Alsanie, "Radio propagation path loss models for 5G cellular networks in the 28 GHz and 38 GHz millimeter-wave bands," *IEEE Commun. Mag.*, vol. 52, no. 9, pp. 78–86, Sep. 2014.
[43] J. H. Kotecha and A. M. Sayeed, "Transmit signal design for optimal estimation of correlated MIMO channels," *IEEE Trans. Signal Process.*, vol. 52, no. 2, pp. 546–557, Feb. 2004.
[44] T. T. Cai and L. Wang, "Orthogonal matching pursuit for sparse signal recovery with noise," *IEEE Trans. Inf. Theory*, vol. 57, no. 7, pp. 4680–4688, Jul. 2011.
[45] J. A. Tropp and S. J. Wright, "Computational methods for sparse solution of linear inverse problems," *Proc. IEEE*, vol. 98, no. 6, pp. 948–958, Jun. 2010.
[46] Y. Shim, W. Choi, and H. Park, "Beamforming design for full-duplex two-way amplify-and-forward MIMO relay," *IEEE Trans. Wireless Commun.*, vol. 15, no. 10, pp. 6705–6715, Oct. 2016.

DEEPA JAGYASI (S'16) received the B.E. degree in electronics and telecommunication engineering from Pune University, Pune, India, in 2010, and the M.E. degree in electronics and communication engineering from Mumbai University, Mumbai, India, in 2013. She is currently pursuing the Ph.D. degree in electronics and communication engineering with the International Institute of Information Technology, Hyderabad, India. Her research interests include millimeter-wave communications, multiple-input-multiple-output precoding, and robust optimization.

P. UBAIDULLA (S'05–M'12–SM'15) received the B.Tech. degree in electronics and communication engineering from the National Institute of Technology (NIT), Kozhikode, in 1997, the M.E. degree in communication engineering from NIT, Trichy, in 2001, and the Ph.D. degree in electrical communication engineering from the Indian Institute of Science, Bengaluru, India, in 2011. He was in the industry, where he focused in the field of radar and sonar signal processing. From 2011 to 2013, he was a Post-Doctoral Fellow with the Computer, Electrical and Mathematical Sciences and Engineering Division, King Abdullah University of Science and Technology, Saudi Arabia. He is currently an Assistant Professor with the International Institute of Information Technology, Hyderabad, India. His current research interests are in millimeter-wave communications and wireless energy transfer.